REPORT DOCUMENTATION PAGE

Form Approved OMB NO. 0704-0188

1. REPORT DATE (DD-MM-YYYY)	2. REPORT TYPE	3. DATES COVERED (From - To)
05-11-2013	Final Report	10-Apr-2013 - 9-Oct-2013

4. TITLE AND SUBTITLE
Real-time label-free detection of suspicious powders using non-contact optical methods

5a. CONTRACT NUMBER

5b. GRANT NUMBER
W911NF-13-C-0052

5c. PROGRAM ELEMENT NUMBER
665502

6. AUTHORS
William F. Hug, Rohit Bhartia, and Ray D. Reid

5d. PROJECT NUMBER

5e. TASK NUMBER

5f. WORK UNIT NUMBER

7. PERFORMING ORGANIZATION NAMES AND ADDRESSES
Photon Systems, Inc.
1512 Industrial Park Street

Covina, CA 91722 -3417

8. PERFORMING ORGANIZATION REPORT NUMBER

9. SPONSORING/MONITORING AGENCY NAME(S) AND ADDRESS (ES)
U.S. Army Research Office
P.O. Box 12211
Research Triangle Park, NC 27709-2211

10. SPONSOR/MONITOR'S ACRONYM(S)
ARO

11. SPONSOR/MONITOR'S REPORT NUMBER(S)
63665-LS-SB1.2

12. DISTRIBUTION AVAILIBILITY STATEMENT
Approved for Public Release; Distribution Unlimited

13. SUPPLEMENTARY NOTES
The views, opinions and/or findings contained in this report are those of the author(s) and should not contrued as an official Department of the Army position, policy or decision, unless so designated by other documentation.

14. ABSTRACT
In situ assessment of suspicious powders within inorganic matrices, with particular emphasis on powders of biological origin, is currently limited to detection by biochemical methodologies that react with monomers such amino acids, nucleic acids, lipids or macromolecule compounds comprised of these basic subunits. These current methods include immunoassays or PCR, both of which require expensive equipment and reagents with limited shelf life and restrictive conditions for storage and use, and considerable time. Current optical methods such as Raman spectroscopy using excitation in the near IR at 785 nm or visible at 532 nm, have not been able to detect or

15. SUBJECT TERMS
Suspicious powders, deep UV, Raman, fluorescence, chemometrics, biological powders, hand-held

16. SECURITY CLASSIFICATION OF:			17. LIMITATION OF ABSTRACT	15. NUMBER OF PAGES	19a. NAME OF RESPONSIBLE PERSON
a. REPORT	b. ABSTRACT	c. THIS PAGE			William Hug
UU	UU	UU	UU		19b. TELEPHONE NUMBER 626-967-6431

Report Title

Real-time label-free detection of suspicious powders using non-contact optical methods

ABSTRACT

In situ assessment of suspicious powders within inorganic matrices, with particular emphasis on powders of biological origin, is currently limited to detection by biochemical methodologies that react with monomers such amino acids, nucleic acids, lipids or macromolecule compounds comprised of these basic subunits. These current methods include immunoassays or PCR, both of which require expensive equipment and reagents with limited shelf life and restrictive conditions for storage and use, and considerable time. Current optical methods such as Raman spectroscopy using excitation in the near IR at 785 nm or visible at 532 nm, have not been able to detect or distinguish biological materials. Until recently, these have been the only classes of handheld instrumentation available to address the problem of identifying suspicious powders in near real-time and in situ at the site of an incident.

We propose to develop and demonstrate an emerging handheld technology that employs a fusion of deep UV excited Raman and fluorescence spectroscopic methods that enable real-time, in situ, detection and classification of trace amounts of biological material: without the need for reagents, labels or other consumables; without contact or disturbing the suspicious powder and subsequent need for decontamination of instrumentation or spread of the powder.

Enter List of papers submitted or published that acknowledge ARO support from the start of the project to the date of this printing. List the papers, including journal references, in the following categories:

(a) Papers published in peer-reviewed journals (N/A for none)

Received Paper

TOTAL:

Number of Papers published in peer-reviewed journals:

(b) Papers published in non-peer-reviewed journals (N/A for none)

Received Paper

TOTAL:

Number of Papers published in non peer-reviewed journals:

(c) Presentations

Number of Presentations: 0.00

Non Peer-Reviewed Conference Proceeding publications (other than abstracts):

Received Paper

TOTAL:

Number of Non Peer-Reviewed Conference Proceeding publications (other than abstracts):

Peer-Reviewed Conference Proceeding publications (other than abstracts):

Received Paper

TOTAL:

Number of Peer-Reviewed Conference Proceeding publications (other than abstracts):

(d) Manuscripts

Received Paper

TOTAL:

Number of Manuscripts:

Books

Received Paper

TOTAL:

Patents Submitted

Patents Awarded

Awards

Graduate Students

NAME	PERCENT_SUPPORTED

FTE Equivalent:
Total Number:

Names of Post Doctorates

NAME	PERCENT_SUPPORTED

FTE Equivalent:
Total Number:

Names of Faculty Supported

NAME	PERCENT_SUPPORTED

FTE Equivalent:
Total Number:

Names of Under Graduate students supported

NAME	PERCENT_SUPPORTED

FTE Equivalent:
Total Number:

Student Metrics

This section only applies to graduating undergraduates supported by this agreement in this reporting period

The number of undergraduates funded by this agreement who graduated during this period: 0.00

The number of undergraduates funded by this agreement who graduated during this period with a degree in science, mathematics, engineering, or technology fields:..... 0.00

The number of undergraduates funded by your agreement who graduated during this period and will continue to pursue a graduate or Ph.D. degree in science, mathematics, engineering, or technology fields:..... 0.00

Number of graduating undergraduates who achieved a 3.5 GPA to 4.0 (4.0 max scale):..... 0.00

Number of graduating undergraduates funded by a DoD funded Center of Excellence grant for Education, Research and Engineering:..... 0.00

The number of undergraduates funded by your agreement who graduated during this period and intend to work for the Department of Defense 0.00

The number of undergraduates funded by your agreement who graduated during this period and will receive scholarships or fellowships for further studies in science, mathematics, engineering or technology fields:..... 0.00

Names of Personnel receiving masters degrees

NAME

Total Number:

Names of personnel receiving PHDs

NAME

Total Number:

Names of other research staff

NAME PERCENT_SUPPORTED

FTE Equivalent:
Total Number:

Sub Contractors (DD882)

Inventions (DD882)

Scientific Progress

See attachment below

Technology Transfer

REPORT DOCUMENTATION PAGE

Form Approved
OMB No. 0704-0188

1. AGENCY USE ONLY *(Leave blank)*	2. REPORT DATE	3. REPORT TYPE AND DATES COVERED
	November 5, 2013	Final Report: 10 April 2013 to 7 October 2013

4. TITLE AND SUBTITLE
Real-time label-free detection of suspicious powders using non-contact optical methods

5. FUNDING NUMBERS
W911NF-13-C-0052

6. AUTHORS
William F. Hug, Ray D. Reid, Rohit Bhartia

7. PERFORMING ORGANIZATION NAME(S) AND ADDRESS(ES)
Photon Systems
1512 Industrial Park St.
Covina, CA 91722

8. PERFORMING ORGANIZATION REPORT NUMBER
W911NF-13-C-0052- Final

9. SPONSORING/MONITORING AGENCY NAME(S) AND ADDRESS(ES)
US Army RDECOM ACQ CTR – W911NF
4300 S. Miami Blvd.
Durham, NC 27703

10. SPONSORING/MONITORING AGENCY REPORT NUMBER

11. SUPPLEMENTARY NOTES

12a. DISTRIBUTION/AVAILABILITY STATEMENT

12b. DISTRIBUTION CODE

13. ABSTRACT (Maximum 200 words)

In situ assessment of suspicious powders within inorganic matrices, with particular emphasis on powders of biological origin, is currently limited to detection by biochemical methodologies that react with monomers such amino acids, nucleic acids, lipids or macromolecule compounds comprised of these basic subunits. These current methods include immunoassays or PCR, both of which require expensive equipment and reagents with limited shelf life and restrictive conditions for storage and use, and considerable time. Current optical methods such as Raman spectroscopy using excitation in the near IR at 785 nm or visible at 532 nm, have not been able to detect or distinguish biological materials. Until recently, these have been the only classes of handheld instrumentation available to address the problem of identifying suspicious powders in near real-time and in situ at the site of an incident.

We propose to develop and demonstrate an emerging handheld technology that employs a fusion of deep UV excited Raman and fluorescence spectroscopic methods that enable real-time, in situ, detection and classification of trace amounts of biological material: without the need for reagents, labels or other consumables; without contact or disturbing the suspicious powder and subsequent need for decontamination of instrumentation or spread of the powder.

14. SUBJECT TERMS
Suspicious powders, deep UV, Raman, fluorescence, chemometrics, biological powders, hand-held

15. NUMBER OF PAGES
33

16. PRICE CODE

17. SECURITY CLASSIFICATION OF REPORT	18. SECURITY CLASSIFICATION OF THIS PAGE	19. SECURITY CLASSIFICATION OF ABSTRACT	20. LIMITATION OF ABSTRACT
Non-Classified	Non-Classified	Non-Classified	UL

Table of Contents

Statement of Problem Studied

Suspicious powder incidents continue to be a disruptive and costly problem for society. In situ assessment of suspicious powders within inorganic matrices, with particular emphasis on powders of biological origin, is currently limited to detection by biochemical methodologies that react with monomers such amino acids, nucleic acids, lipids or macromolecule compounds comprised of these basic subunits. These current methods include immunoassays or PCR, both of which require expensive equipment and reagents with limited shelf life and restrictive environmental conditions for storage and use. These methods also require high skill levels. Current optical methods such as Raman spectroscopy using excitation in the near IR at 785 nm or visible at 532 nm, have not been able to detect or distinguish biological materials from background or other materials. Until recently, these have been the only classes of handheld instrumentation available to address the problem of identifying suspicious powders in near real-time and in situ at the site of an incident.

The goal of this project is to develop and demonstrate an emerging handheld technology that employs a fusion of deep UV excited Raman and fluorescence spectroscopic methods. The proposed low cost handheld Biological Reconnaissance & Analysis using Non-Contact Emission-spectroscopy (BRANE) sensor enables detection and classification of a broad range of suspicious powders in real-time at the site of a contamination incident:

1. without the need for reagents, labels, or other consumables;
2. without contact with or disturbing the suspicious powder and the subsequent need for decontamination of the sensor or spreading, growing, or dispersing biological threats in suspicious powders;
3. with rapid analysis- for each 60 μs laser pulse a full spectrum analysis is possible. Dwelling on a sample for 5 to 10 seconds can dramatically improve signal to noise of data for weak signals.

The BRANE sensor eliminates the cost and logistics associated with single-use label kits needed by current immunoassay and PCR based methods. The BRANE sensor has the non-contact, no sample handling advantages of Raman based sensors, but has the advantages of deep UV excitation of samples at wavelengths that enable simultaneous detection of both Raman emissions without obscuration by fluorescence and fluorescence emissions without alteration by Raman emissions. This can only be conducted in the deep UV below 250 nm. The handheld BRANE sensor is capable of making **millions of tests with no consumables cost** in an instrument with indefinite field lifetime. The BRANE sensor is also capable of detection and classification of a much broader range of contaminants beyond biological that includes chemical and explosives hazards. All this is done in a single sensor without the need for modification for different applications.

The BRANE sensor is best described as a "disruptive technology" that approaches biological threat analysis using a unique paradigm – optically analyze the nucleic, protein, and lipid components of biological threats to assess their presence and identity. This is enabled by three new technology elements: a unique, new, miniature deep UV laser with narrow linewidth which enables simultaneous Raman and

fluorescence detection; a new high speed linear CCD array detector which enables handheld miniaturization; and new chemometric algorithms which enable classification of biological material using a fusion of deep UV Raman and fluorescence spectroscopy.

Summary of Important Results of Phase I SBIR

This is the final report on this Phase I SBIR contract. During this six-month effort, we developed and demonstrated the ability to detect and differentiate trace amounts of different microbes from a wide range of organic and inorganic materials using a unique, new technology, hand held instrument weighing about 7 pounds including batteries for many hours of use, with a present 1st generation size about 4" wide by 9" high by 16" deep.. The low cost handheld Biological Reconnaissance & Analysis using Non-contact Emission-spectroscopy (BRANE) sensor enables detection and classification of a broad range of suspicious powders in real-time at the site of a contamination incident:

1. without the need for reagents, labels, or other consumables;
2. without contact with or disturbing the suspicious powder and the subsequent need for decontamination of the sensor or spreading, growing, or dispersing biological threats in suspicious powders.
3. with rapid analysis- for each 60 μs laser pulse a full spectrum analysis is possible. Averages of 400 pulses (10 seconds) enables enhanced signal to noise, especially for weak Raman emissions.

The fundamental science that enables the ability to differentiate a wide range of CBE materials is deep UV excited Raman and fluorescence spectroscopy where Raman and fluorescence emissions from an unknown sample occur in distinctly separate spectral bands and thereby do not obscure or alter each form of emitted radiation. Operating at excitation wavelengths below 250 nm, both Raman and fluorescence emissions can be collected simultaneously on a single array detector, with Raman emissions providing information about molecular bonds with the unknown sample, and fluorescence emissions providing information about overall electronic structure of the sample. This cannot be accomplished using excitation at wavelengths above 250 nm, including common laser wavelengths at 263 nm, 266 nm, or longer wavelengths, where fluorescence from the sample or its matrix often completely obscure Raman emissions and also alter fluorescence emissions due to strong Raman bands. The combined use of Raman and fluorescence spectroscopy conducted in the deep UV has been patented by Photon Systems and enables a rich spectral and chemometric description of unknown samples.

The fundamental technologies that enable this new capability to differentiate CBE materials in a small instrument are: 1) new technology low cost deep UV lasers, also developed and patented by Photon Systems, that provide high power and energy in a small, 1 pound, low power consumption package; and 2) new technology resistive gate linear CCD array detectors developed by Hamamatsu Corp. that enable room temperature operation due to their fast array readout, allowing now dark noise accumulation. In addition, during the Phase I effort, Photon Systems developed a custom circuit board and firmware to interface the new Hamamatsu CCD array detector to a previously developed on-board imbedded microprocessor and memory system that controls the sensor and provides on-board data processing and display of the chemometric information in the BRANE sensor. Integrated in the BRANE sensor will be an onboard library of known biological, organic, and inorganic materials with which to compare unknown suspicious powder spectral data. Each "interrogation" of a sample will lead to an identification of the suspicious powder and a probability that the unknown powder is a material in the on-board library.
During the Phase I effort, we obtained deep UV Raman and fluorescence spectra of a wide range of materials using both laboratory and hand-held engineering model instruments using the core enabling laser and detector technologies represented in the BRANE sensor. These materials included the biological materials B. subtilis, E. coli, P. aruginosa, and S. cereviciae as well as a wide range of possible interferent or confusant organic materials such as powdered sugar, granulate sugar, fruit pectin, flower, corn starch, baking powder, baking soda, aspirin, Aleve, and acetaminophen, as well as inorganic

interferent or confusant materials such as calcium and sodium borate, calcite, Ca/Mg carbonate, rhodochrosite, dolomite, siderite, augite, quartz in many forms, gypsum, BaSO4, Kaolinite, and talc.

From the deep UV Raman and fluorescence data taken to date we developed and demonstrated algorithms for triaging a suspicious powder in seconds with a 4 step process to progressively elaborate understanding of the powder, starting with the baseline bio/non-bio identification to subsequent further elaboration of the form of biological threat posed by the powder. We also developed hardware, firmware, and software designs of a compact, fully integrated, hand-held instrument satisfying the goals of this project. And finally, we began construction of the first generation model of the BRANE instrument, shown in Fig. 1 below.

As further demonstration of the unique capability of the science and technology represented in the BRANE sensor, a larger predecessor instrument to BRANE developed under earlier programs have been independently tested at Lawrence Livermore National Laboratory (LLNL), University Multispectral Laboratories (UML), and NAVEODTECHDIV. In all cases, our patented deep UV Raman and fluorescence lasers and detection technology was determined to be superior to all other methods tested, notably near IR Raman sensors, FTIR, and other methods. The most recent tests are ongoing at NAVEODTECHDIV where a deep UV fluorescence-only version of our sensor, described as the TUCBE FX, was the only sensor out of a wide variety of sensors and methods to move on to Phase II testing. This biological testing is ongoing at the time of this report at Dahlgren, VA.

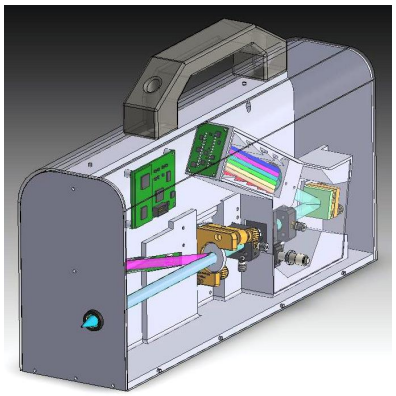

Figure 1. SolidWorks drawing of 1st generation model of BRANE sensor: 7 lb., 4"w, 9" h, 16" d

Task 1: Microbial differentiation using deep UV Raman & fluorescence

The goal of this task was to assess the benefits of combined Raman and native fluorescence versus separate Raman or native fluorescence as a means to enable microbial classification. Preliminary data collected on a series of microbes suggest that differentiability can be achieved using fluorescence alone.

During the Phase I effort a large amount of Raman and fluorescence data was taken on a wide range of samples and instruments. These data were essential to the development of the BRANE instrument design illustrated in Fig. 1. A significant amount of effort was also involved in sample preparation to ensure accurate data. Sample preparation procedures and instruments and spectral data will be described in detail in Appendices A and B at the end of this report in order keep the focus on the body of this report on interpretation of the results and sensor design and the significance of the BRANE instrument for detection and identification of a wide range of trace and bulk chemicals in a very small, hand-held instrument.

1.1 Triaging suspicious powders

During the Phase I effort, we developed a tiered approach to sample analysis that employed deep UV fluorescence and deep UV Raman spectroscopy. We identified biochemical drivers for a process of triaging samples to provide higher and higher levels of sample differentiability & characterization enabled by each subsequent analysis. **We demonstrated that high-resolution deep UV fluorescence spectroscopy alone is capable of differentiating benign suspicious powders from microbes and determine which types of microbes are present (bacterial cells, bacterial spores, yeast).** The presented analyses use spectral data that include: 1) pure microbes dried on a surface; 2) microbes mixed into an inorganic (Talc) at or below concentrations required by the program (1000:1 and 10,000:1 of inorganic to microbes by mass); and 3) potential interferent or confusant materials such as other white inorganic *and organic* powders that are non-hazardous but may be used in a hoax.

A progressive analysis flow diagram is shown in Fig. 2. This flow diagram focuses on the capability of the BRANE sensor as it has presently evolved – focusing on the high resolution fluorescence spectra while maintaining the ability to add a wider range of Raman data in future enhancements. Using high resolution deep UV fluorescence offers a BRANE sensor that is compact, low-cost, low-power, and easy-to-use and that can be used for millions of sample analyses without service or consumables, i.e. negligible cost per test.

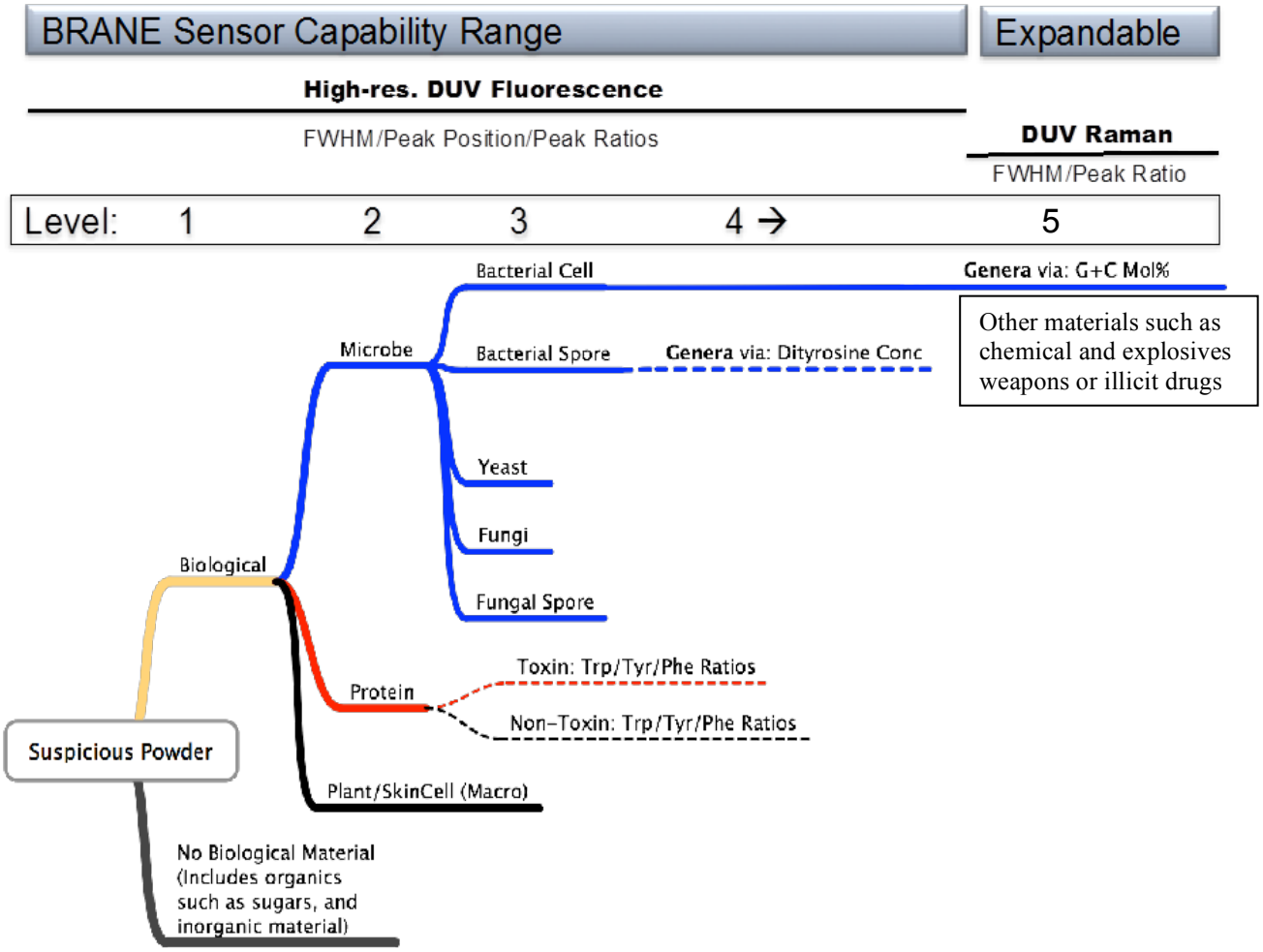

Figure 2. Graphical representation of Level 1 – 5 sample triage capabilities of the BRANE sensor. This diagram shows the extent of detection differentiability using fluorescence spectra and shows where deep UV Raman spectra provides an enhancing capability. The BRANE sensor design is currently focused on the spectral region from 270 nm to 400 nm, however it is being designed with the intent to be able to incorporate enhanced deep UV Raman in future generations if the operational scenarios require it.

In discussions with Dr. W. Buchholz of ARO at the program kickoff, our SBIR effort was to focus on the ability differentiate biological from non-biological material. Biological material includes microbes, proteins, as well as plant and skin cells. Non-biological material incudes a long list of organic and inorganic materials that are potential interferents and confusants. This is the lowest level of analysis, Level 1 in Fig. 2, for the BRANE sensor. Level 1 requirements can be obtained by low-resolution or high-resolution fluorescence spectra. However the high resolution fluorescence configuration of the BRANE sensor, with the same laser and detector, can be used to provide much more information, including

materials listed in Fig. 2 at Level 2 and 3, as well as possible Level 4 information. After evaluating all instrument options, we have focused our development only on the high spectral resolution version of BRANE. As such, for the remainder of this report, only the high-resolution data will be discussed.

Level 1 Analysis

To demonstrate the instruments' ability to achieve Level 1 bio/non-bio requirements, high-resolution fluorescence data on a number of different organic and inorganic materials were compared against a number of different microbes using Principal Component Analysis (PCA). Care was taken to ensure that all microbes were vetted to be pure and well washed of media. This process is described in detail in Appendix A at the end of this report. While details of calculations for PCA are outside the scope of the report, the basic premise is that PCA re-represents the spectra in terms of Principal Components (PC). Each PC states a weighting for each spectral bin (pixel), which are applied to each spectrum in the input dataset and summed to provide a single value for a PC. Weights for each PC are determined by the algorithm and are dependent on the variance of the input dataset, i.e., if the dataset changes, and that change increases or decreases the variance in the data, the weights for each PC will change. The PCs, when output, are ranked in order of the weightings that accentuate the spectral regions that have the greatest variance. However it is not necessarily the first PC should be used – the choice of PCs to use requires analysis of the weights to ensure that they are not accentuating instrument artifacts or other non-chemical related features.

It should be noted that PCA is not a cluster algorithm. Rather it is a method by which high resolution data can be compared to quickly assess which spectral regions, if any, provide chemical separation or differentiability. It should also be noted that all the separations stated here are traced back to chemistry by looking at the weightings and extrapolating the chemical nature that is driving the separation.

Inorganic Materials
Calcium Borate
Sodium Borate
Ca/Na Borate
Calcite
Ca/Mg Carbonate
Rhodochrosite(xtal)
Rhodochrosite(powder)
Dolomite
Siderite
Augite
Quartz (coarse)
Quartz (fine)
Quartz (baked)
Quartz (xtal)
Quartz (xtal MeOH cleaned)
Quartz (powder baked)
Gypsum
BaSO4
Kaolinite
Talc

Organic Powders
Baking Powder
Powdered Sugar
Baking Soda
Fruit Pectin
Flour
Cornstarch
Aspirin

Microbe Standards
B. subtilis
E. coli
S. cereviciae
P. aeruginosa

Representative Spectra

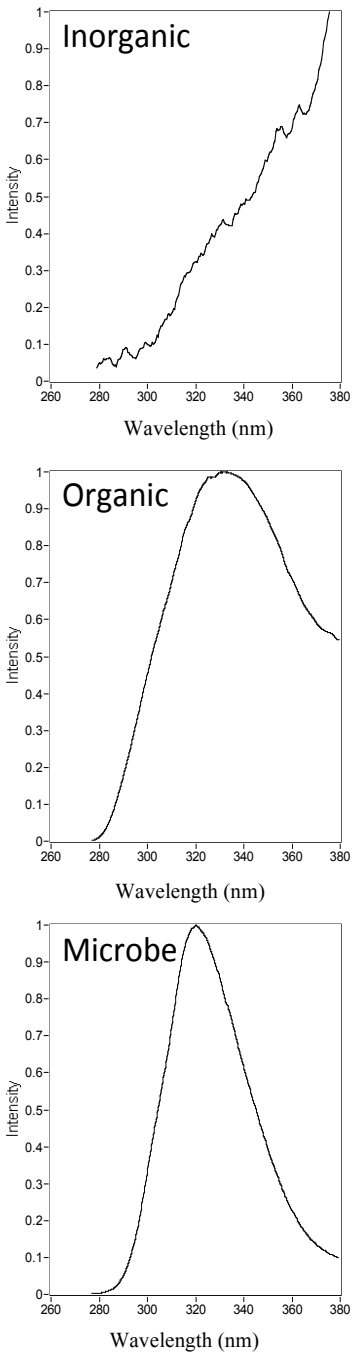

Table 1. List of materials used in the analysis. Representative spectra are shown. In addition to the microbe standards, dilutions were made in talc with a 1,000:1 and 10,000:1 inorganic to organic ratio.

The results of the Level 1 PCA analysis are show in Fig. 3 with the input from samples stated in Table 1. The PCA "space", i.e. the weights for the PCs, were determined by a training set that included the dried, cleaned, pure microbes and the inorganic components only. Analysis of the weights suggested that PC1 and 2 were correlated and were weighing the same spectral regions but in an inverse manner, therefore, PC2-4 were used (PC1 was ignored). Figure 3 show PC2 vs PC3 and PC2 vs P4 as 2-D plots to simplify the visualization of what would normally be a 3D plot.

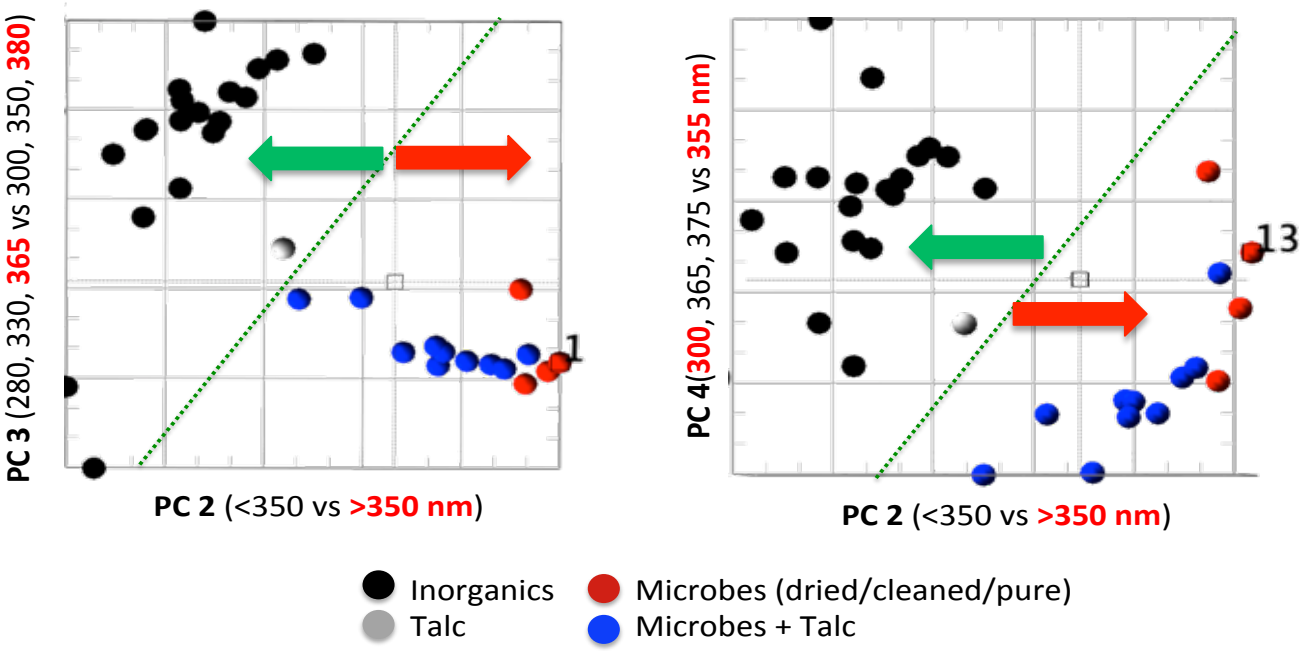

Figure 3. PCA plots for PCs 2-4 of inorganics, microbes (pure), and microbes+inorganics at dilutions of 1000:1 of inorganic to bacteria. The Green-dotted line represents a simple plane that separate the inorganic versus microbe containing material. The PCs that form the X and Y axes include the spectral bands that have weights assigned to them. The values in red-bold are the most weighted features for that PC.

The plots show that a simple plane (indicated by green dotted line) can be created to differentiate inorganic vs. microbial (black vs red spheres) as well as inorganic vs. microbes+inorganic (black vs blue spheres) at required concentrations; thus demonstration of achieving Level 1 requirements. The green arrows show non-hazard. Red arrows show biological and potentially hazardous.

Analysis of the PC 2, 3, and 4 weights (Fig. 4), and the representative spectra from Table 1 materials, shows that the spectral range from 280 to 380 nm is necessary for differentiation. However adding in organic/biological powders, such as stated in Table 1, the PCA plot, using the PC 2, 3, and 4, cannot differentiate between these organic materials and microbes. Therefore, these weights cannot be used for Level 2 requirements (Fig. 2), where distinction between microbes and other biological compounds are needed. Although this was not stated in the original goals of the program, it became increasingly clear that organic material, either as part of the inorganic or through contamination, may lead to confusion. Since adding the organic powders to the PCA space shows that the majority of materials group with the microbe-containing material, as shown in Fig. 5, the Level 1 process effectively differentiates between inorganic and biological materials. Materials that pass Level 1 to Level 2 (i.e. the sample is either organic or microbial) need to be processed by another analysis test that requires retraining the PCA space.

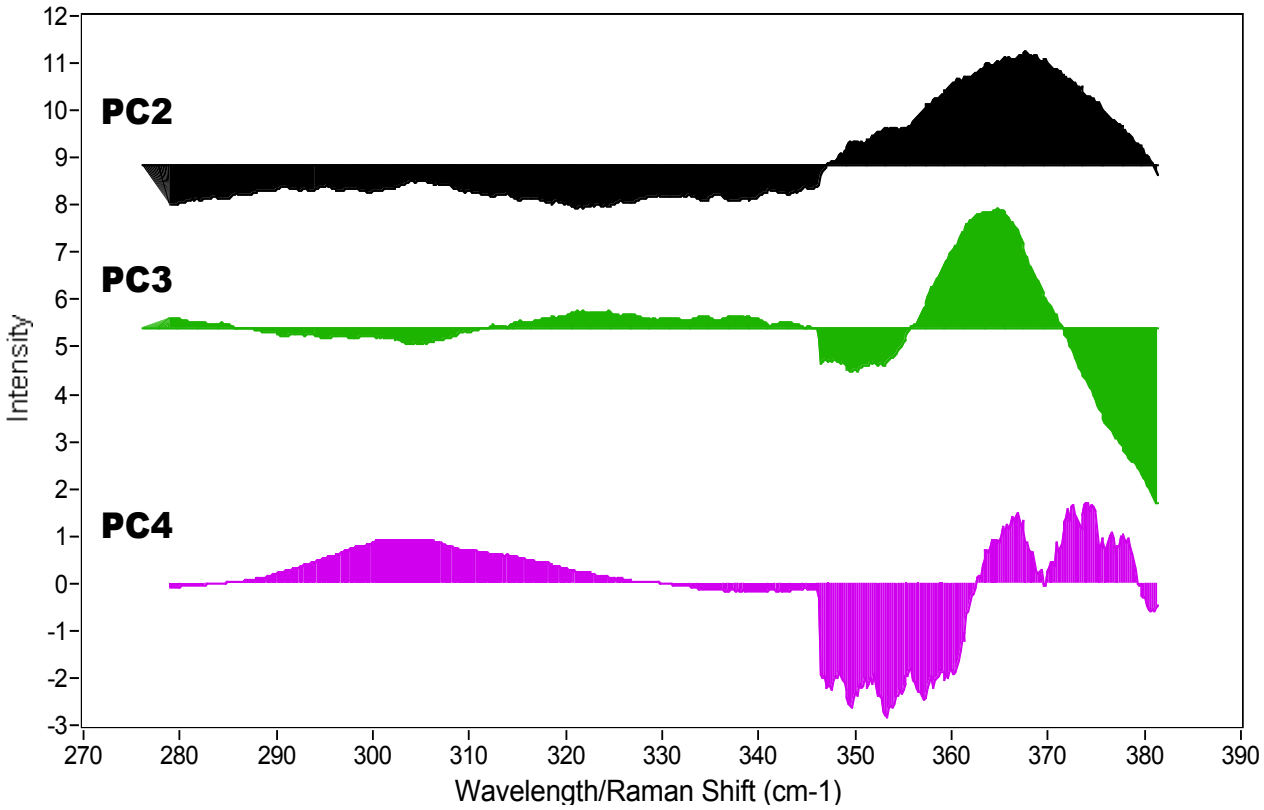

Figure 4. Spectral weightings for PCs 2-4 using inorganics and microbes (pure) to train the PCA space. As can be seen, the weights can be positive and negative.

Level 2 Analysis

The analysis for achieving Level 2 requirements is for differentiation of microbes from proteins and plant and skin cells. *This assumes that the Level 1 analysis has determined that the unknown suspicious powder is biological and is NOT non-biological.* This can be done automatically in a future version of BRANE sensor software. Presently, triage data analyses are being done manually. The samples used for Level 2 analysis are cleaned microbes, proteins, and plant and skin cells. The same spectral data base from these samples was used, after determining the suspicious powder was biological, to re-train the eigenvectors for the PCA. **The re-trained PCA space, with the microbe+inorganic samples, are shown in Fig. 5 where, again, a simple plane can be used to separate microbes and microbial containing material from the organic/biological material; achieving the Level 2 goals.** In this analysis case, only PC2 and PC4 were used (weights shown in Figure 5) and again show that features from the entire spectrum are necessary with different weightings to those used in the Level 1 analysis.

It should be noted that while PCA is a computer intensive calculation, these calculations will not need to be performed on the instrument. It is expected that as the database of materials expands, the weights to perform these separations will be refined and calculated offboard the sensor. BRANE analysis in the field would only require the use of the training set weights for each Level. As such the calculations for this process are simple and can be performed on an embedded processor and/or a small FPGA.

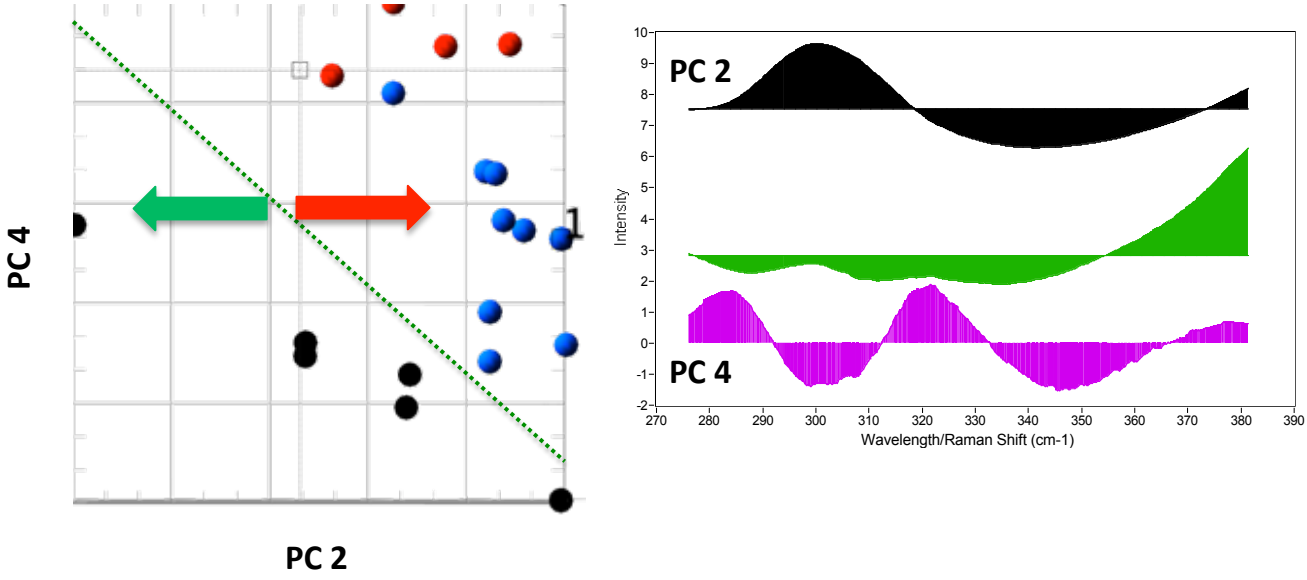

Figure 5. PCA with retrained space for Level 2 requirements; only PC2 and PC4 are needed. Black spheres in this case are the organic powders (Table 1). Red spheres are pure microbes and blue spheres are microbes+inorganics in a wide range of solid/solid dilutions down to 1/10,000. The only data input into this space are materials that pass through Level 1 analyses. Weightings for the PC2 & PC4 are shown on the right.

Level 3 Analysis

At the Level 3 of specificity, the BRANE sensor needs to be able to accurately and rapidly differentiate bacterial cells, bacterial spores, yeast, fungi, and fungal spores. At this level, the sensor also potentially needs to be able to classify protein toxicity based on Trp/Tyr/Phe ratios. This has also been demonstrated to be possible using broadband deep UV fluorescence methods. At Level 3, you will note in Fig. 1 that the solid lines in the flow diagram start to change from solid lines to dashed lines. Solid lines indicate what has been demonstrated. Dashed lines indicate what appears to be possible but which has not yet been confirmed. At the third level of specificity, the detection method begins to migrate from a broadband deep UV fluorescence-only instrument to an instrument that is still fluorescence-only but incorporates higher spectral resolution fluorescence measurements, typically less than 1 nm. Using the higher resolution, room temperature, resistive gate linear CCD array, the BRANE sensor SWAP decreases along with a decrease in sensitivity, but the information content and related specificity increases. The BRANE sensor, as proposed, with the room temperature linear CCD array detector, is still extremely sensitive and can detect very small quantities of bacteria.

Level 3 analyses again assume that only materials that have passed through Level 1 and 2 analyses can be processed by Level 3 algorithms. In this case, the data only include microbes and microbe containing samples (with concentrations of >10,000:1 ratio of inorganic to microbe). For Level 3 differentiation, the analysis is a bit more simplified and relies on ratios of specific spectral regions that highlight the chemical differences between yeast, bacterial cells, bacterial spores, etc. For example, bacterial spores have 15% dityrosine in their spore coat and have a characteristic spectral feature at ~300 nm when excited at <250 nm[1]. Comparatively, bacterial cells have a more pronounced 320 - 330 nm feature; stemming from higher concentration of tryptophan in the cell wall proteins. As such, the "algorithms" used for Level 3 used spectral regions at 300 nm and 310 nm with ±5 nm bandwidths (Fig. 6).

[1] Bhartia, Rohit, William F Hug, Everett C Salas, Ray D Reid, Kripa K Sijapati, Alexandre Tsapin, William Abbey, Kenneth H Nealson, Arthur L Lane, and Pamela G Conrad. 2008. "Classification of organic and biological materials with deep ultraviolet excitation." *Applied spectroscopy* 62(10): 1070–1077.

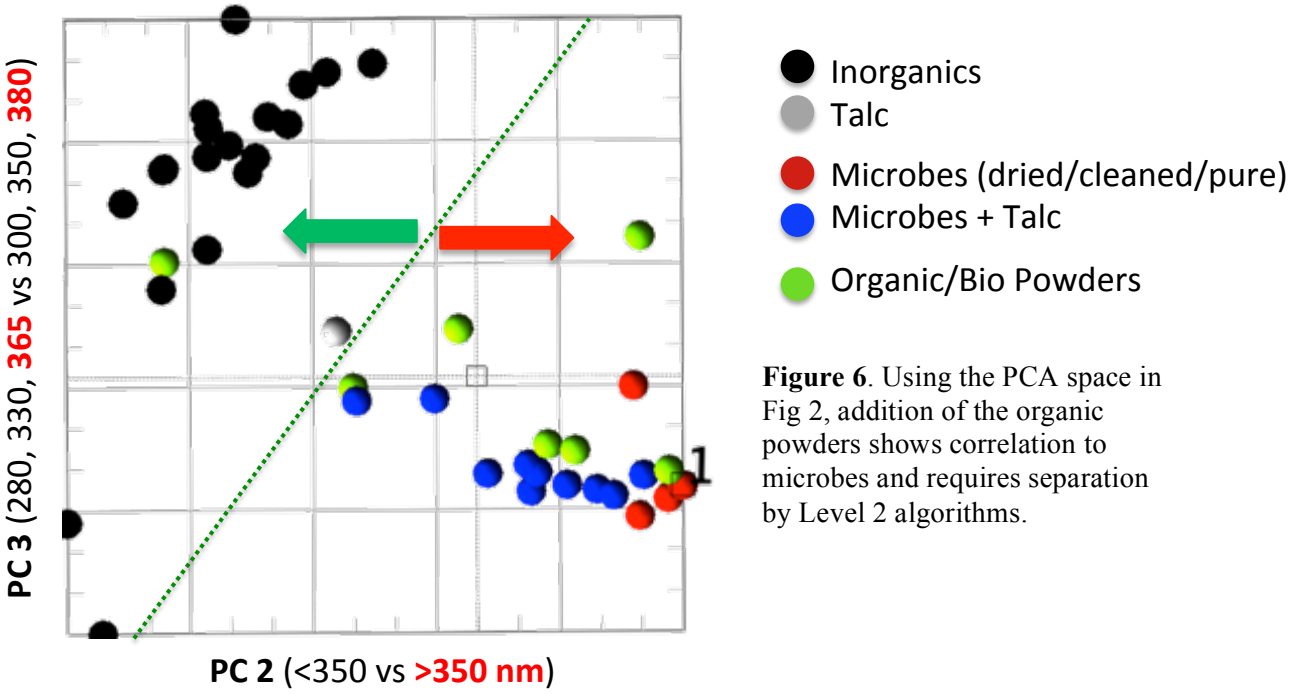

Figure 6. Using the PCA space in Fig 2, addition of the organic powders shows correlation to microbes and requires separation by Level 2 algorithms.

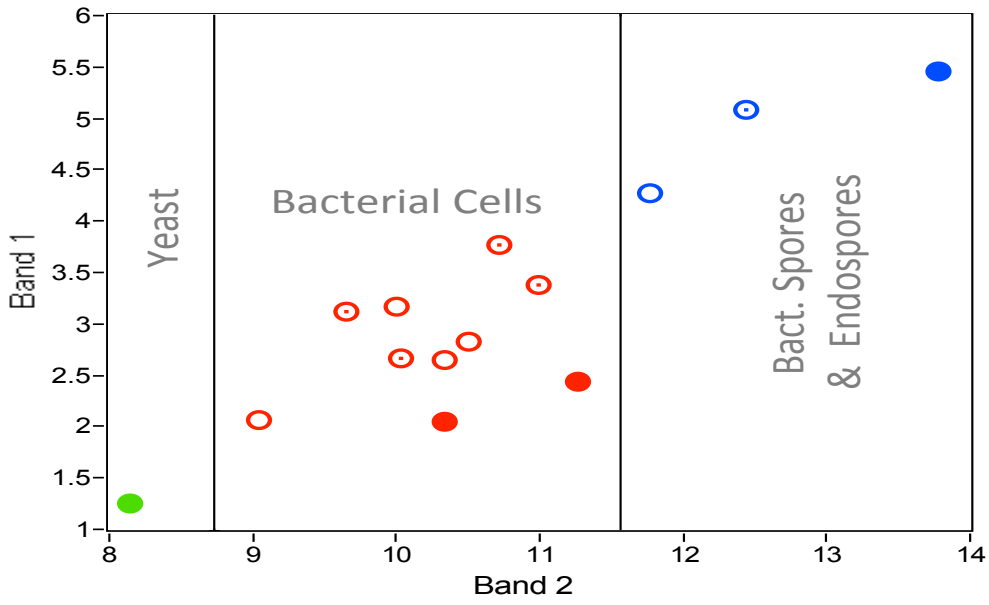

Band 1: 300± 5nm
Band 2: 310± 5nm

Solid Circles: Dried Microbial Samples
Open Circles: 1000:1 inorganic:microbes dilution
Dotted Circles: 10,000:1 inorganic:microbes dilution

Figure 7. Band comparison. The solid circles (pure microbes) were used to establish placement of the discriminators. The addition of microbial/inorganic dilutions categorize all the samples correctly. The only data input to this analysis were materials that passed the Level 1 and 2 tests.

In the Level 3 analysis, the materials comprising the microbe group, yeast, bacterial cells, and bacterial spores/endospores are easily separated using 2 linear discriminators in a scatter plot of the two selected band regions. This is shown in Fig. 7. These were established using only the pure materials and then the inorganic:microbical dilutions were added. **These analyses demonstrate successful differentiation for Level 3 analyses.**

The Level 1-3 analyses have only used deep UV fluorescence spectroscopy (with excitation <250nm) and has demonstrate the ability to differentiate between inorganic, organic, microbes, microbes/inorganic dilutions and down the bacterial cell/spore and yeast level. These have been demonstrated using three separate algorithms, specific to each Level.

Level 4 Analysis

At Level 4 of specificity, the BRANE sensor needs to be able to differentiate different genera of bacterial spores, cells, yeasts, etc. We have demonstrated, even with lower spectral resolution fluorescence the ability to distinguish different genera, but the higher spectral resolution improves this ability. The increased resolution is provided by the linear CCD array detector. The improved specificity is enabled because of the indirect relationship between Tyr/Phe content of cells to the G+C Mol% of different bacteria. The spectrum for each microbe is unique and dependent on the ratios of tryptophan (Trp), tyrosine (Try), and phenylalanine (Phe) [Ref.1]. Furthermore, Phe and Tyr concentrations are strongly dependent on G+C% content in bacterial cells[2]. This tie between Tyr and Phe with G+C% content is a key component of how native fluorescence contributes to bacterial identification. Since G+C% content is conserved within species but not within genera and can act as a means of taxonomic classification[3]. Two CDC Cat A bacterial cells, Y. *pestis* and F. *tularensis* have GC contents of 47%[4] and 32.9%[5] respectively. According to Lobry 1997, the 15% variation in GC content would suggest that the Phe and Tyr content is higher for F. *tularensis* than Y. *pestis*. Note, that the variation in GC content for S. subtilis (44%), E. *coli* (51%) and P. *aeruginosa* (63%) are similar to that of F. *tularensis* than Y. *pestis* and as such show B. subtilis and E coli with an increased Tyrosine content. Some of these effects on native fluorescence spectra are shown below.

Figure 8 is an illustration of the ability to differentiate different dilute streaks of microbes on a stainless steel substrate, including B. subtilis, E. coli, P. aruginosa, and S. oneidensis. This was accomplished using a sensor which we call at Targeted Ultra Violet Chemical Sensor (TUCS) with 6 independent, 20 nm wide, fluorescence channels centered at 280 nm,, 300 nm, 320 nm, 340 nm, 360 nm, and 380 nm, mounted on a XY scanning stage to enable 6-channel deep UV mapping of the fluorescence emissions from a surface. The color rendition on Fig. 8 is determined by the RGB position in a chemometric space determined by a band difference analysis (BDA) method in which RGB are the coordinates of band

---

[2] Lobry, JR. 1997. "Gene : Influence of genomic G + C content on average amino-acid composition of proteins from 59 bacterial species." *Gene* (205): 309–316.

[3] Wayne, L G, D J Brenner, R R Colwell, PAD Grimont, O Kandler, M I Krichevsky, L H Moore, WEC Moore, RGE Murray, and E. Stackebrandt. 1987. "Report of the ad hoc committee on reconciliation of approaches to bacterial systematics." *International Journal of Systematic Bacteriology* 37(4): 463–464.

[4] Perry, R D, and J D Fetherston. 1997. "Yersinia pestis--etiologic agent of plague.." *Clinical microbiology reviews* 10(1): 35–66.

[5] Larsson, Pär, Petra C F Oyston, Patrick Chain, May C Chu, Melanie Duffield, Hans-Henrik Fuxelius, Emilio Garcia, Greger Hälltorp, Daniel Johansson, Karen E Isherwood, Peter D Karp, Eva Larsson, Ying Liu, Stephen Michell, Joann Prior, Richard Prior, Stephanie Malfatti, Anders Sjöstedt, Kerstin Svensson, Nick Thompson, Lisa Vergez, Jonathan K Wagg, Brendan W Wren, Luther E Lindler, Siv G E Andersson, Mats Forsman, and Richard W Titball. 2005. "The complete genome sequence of Francisella tularensis, the causative agent of tularemia." *Nature Genetics* 37(2): 153–159.

difference between 380-280 nm, 360-300 nm, and 340-320 nm. The amplitude of each of these band differences was used to determine the intensity of R, G, and B in the image.

Because of the liquid streaking method, microbes tended to migrate to the edges of the drying deposit. As a result, especially for BS and PA, where BS is dominated by the greenish color, EC is dominated by the bluish color, PA is dominated by the purple color, and SO is dominated by the blue/green color. Some of the other colors are due to phosphate crystalline features from dried buffer. The white features around the periphery of PA is due to saturation of the detectors. The purpose of this slide was to illustrate the ability to differentiate microbes, even to the eye, using fluorescence excited in the deep UV. We have shown this more analytically in the past using principal component analysis to show the difference in fluorescence spectral features between these microbes. Microbial fluorescence spectra are different than the sum of spectral features of their individual chemical components. This is believed to be due to the conformation of the peptides, proteins, DNA, and other constituents with a whole microbe.

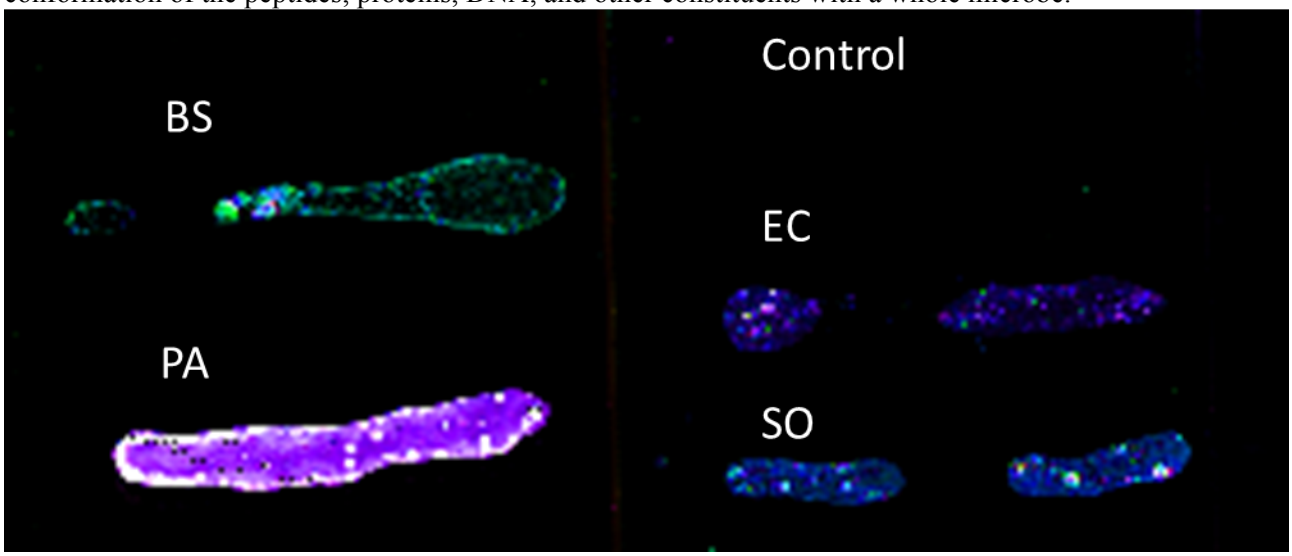

Figure 8. 3-color Band Difference Analysis (BDA) chemometric-space spatial maps of dilute streaks of 4 microbes on a stainless steel substrate. BS= B. subtilis, EC= E. coli, PA= P. aruginosa, and SO= S. cereviciae.

Below, in Fig. 9, are high resolution fluorescence spectra from the inexpensive S11155 CCD array detector planned for the BRANE sensor showing the variation in the leading edge of the fluorescence emission signature of 3 bacteria and one yeast microbes: B. subtilis (44 G+C%), E. coli (51 G+C%), P. aruginosa (64 G+C%), and S. cereviciae (38 G+C%). The bacteria are shown in Fig. 9 where the shortest emission wavelength curve is related to the bacteria with the lowest G+C%, B. subtilus, increasing in wavelength with increasing G+C%. This is an indication of decreasing tyrosine content of cells with increasing G+C% content. The exception is the yeast, which is identified differently. Note that at this there are no Raman emissions evident from this concentration of microbes in the 250 nm to 275 nm spectral range corresponding to 0 to 4000 cm-1 in Raman shift. Only fluorescence emissions are detectable.

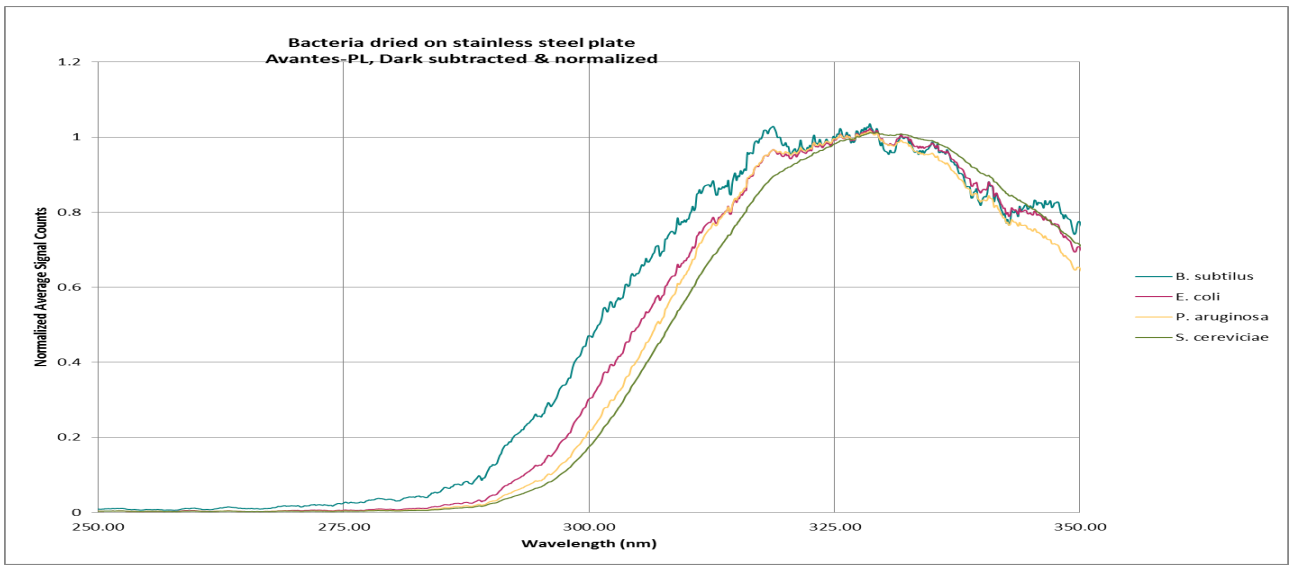

Figure 9. Native fluorescence spectra of microbes of different G+C% content. 248 nm excitation, S11155 detector

Level 5 Analysis

At the present time, we are not convinced that adding a higher level of Raman spectroscopic capability to the BRANE sensor will improve the specificity of identifying different genera or species of bacteria or microbes. The primary additional biological information would be by direct Raman measurement of nucleic acid vibrational modes for A, G, T, and C. This has been demonstrated in several publications by Prof. Wilfred Nelson from the Univ. of Rhode Island in the early 1990's and recently by Prof. Juergen Popp of the Friedrich-Schiller University, Jena, Germany[6,7]. Although we continue to evaluate this method for biological materials, we believe the best advantage of adding enhanced Raman capability to the BRANE sensor is in the expanded ability to detect other important hazardous materials such as chemical and explosive weapons materials as well as illicit drugs.

Because Raman emission is at least 1000x weaker than fluorescence, it is not possible to obtain very good Raman spectra with a room temperature CCD detector. Instead of dwelling on an unknown suspicious powder for less than 1 second, the dwell time can increase to 10s of seconds. At these integration times, dark noise is a major problem for CCD array detectors. As a result, the detector needs to be cooled to enable longer integration or dwell times on an unknown sample, without degrading the signal to noise ratio (SNR) due to dark current and related noise from the detector. The detectors we have used for engineering testing are a liquid nitrogen cooled detector on the 550 mm focal length instrument, and 2 and 3 stage thermoelectrically (TE) cooled detectors on the 260 mm focal length instrument. Each TE cooler stage provides approximately 20 deg C drop in operating temperature below ambient, corresponding to a significant dark noise reduction. TE cooled detectors would improve the performance at Level 5 specificity by improving SNR for both fluorescence and Raman, but without this type of detector, only very strong Raman emissions will be detectable. With this detector, Raman emissions from a much wider range of materials would be detectable, but the sensor detection method is more complicated, with higher Size, Weight, and Power (SWAP) as well as cost. With a cooled CCD detector, it is necessary to run warm-up the instrument for at least 10 to 15 minutes before taking data, at a power consumption level about 50W compared to zero W for the BRANE sensor with uncooled detector. This cuts battery lifetime and/or increases battery size and weight. The cooled detector also is nominally 10 times more expensive,

[6] Schmitt, M., J. Popp, et.al. "Deep UV Raman spectroscopy of biological and mineralogical samples", 39th Annual Meeting, FACSS, Kansas City, MO, paper 381, Oct. 1, 2012
[7] Popp, J. et.al., "Single cell Raman Micro-spectroscopy- a powerful tool in biophotonics", 39th Annual Meeting, FACSS, Kansas City, MO, paper 637, Oct. 1, 2012

going from about $1000 to $10000, for the detector alone, with a commensurate increase in size and weight. These are the driving disadvantages of moving to Level 5. In addition, we have also found that for detection of microbes, deep UV fluorescence is far more effective than Raman methods.

As stated earlier, the current focus for the BRANE instrument is on developing deep UV fluorescence analysis for enabling a low cost instrument to determining whether a suspicious powder is biological or non-biological. With the results presented above, we believe we have demonstrated the ability to achieve and exceed the stated goals of the program by including differentiation between organic/biological powders as well as differentiation of different microbes with better limits of detection using deep UV fluorescence alone.

By pushing the limits of differentiability of biological, organic, and inorganic suspicious powders using deep UV fluorescence alone, the size, weight, power consumption and cost of the BRANE sensor is kept to a minimum. As will be discussed in greater detail below, there is the opportunity to evolve this sensor to include enhanced Raman detection not possible with the low cost detector presently incorporated in the present version of BRANE. Such an enhanced sensor would be slightly larger, have more than double the power consumption and increased cost primarily associated with the focal plane CCD array detector. This is an option what can be discussed as an extension to the Phase II effort.

Task 2: Optomechanical & electronics design of the BRANE sensor

The goal of this task is to develop the BRANE sensor design. The design goal is a rugged, handheld, non-contact analyzer in the smallest package and lowest cost possible design. Our design direction is focused on the integration of our ultra-narrow-linewidth deep UV lasers emitting at 248.6 nm with new technology resistive gate, back thinned, back illuminated, linear CCD array detectors which have very high readout rates and enable detection of weak Raman and fluorescence signals without the need for detector cooling and the associated increased sensor size, weight, and power consumption. This is an essential aspect of the technology innovation that enables the benefits of deep UV excitation in a small handheld package. The core technologies that enable the BRANE sensor are the new technology deep UV laser from Photon Systems (NeCu30) and the new technology high speed linear CCD array detector from Hamamatsu (S11155). Lesser, but also very important, are optical component and coating technologies which are rapidly evolving for deep UV applications.

The NeCu30 laser, developed and patented[8] by Photon Systems, Inc., emits about 250 mW at 248.6 nm with a laser linewidth less than about 2 GHz, corresponding to less than 0.1 cm-1. Emission line stability is less than 1 ppm and is independent of ambient temperature. The laser line is a direct CW laser line which is commutated with pulse width typically about 50 μs. This is adequate energy to make most fluorescence spectra measurements in a single laser pulse. Pulse repetition rates are typically 40 Hz or less so that fluorescence spectra are taken at a high rate of speed, enabling spatial mapping of the suspicious powder distribution on surfaces. The NeCu30 laser is a hollow cathode glow discharge laser weighting about 1 lb and drawing about 12 W at a 40 Hz sample rate and 3 W at a 10 Hz sample rate. NeCu30 lasers are about 500 times smaller, 3000 times lower power consumption, and 100 times lower cost than lasers with similar deep UV optical properties. These lasers have been tested to high levels of shock and vibration and ambient temperature variations and have been on many expeditions to Antarctica, the Arctic, and deep Ocean. These TRL 6 to 7 lasers are the most core of the technologies that enable the BRANE sensor.

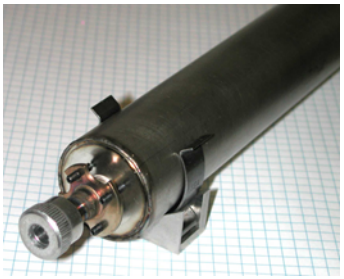

Figure 10. Typical NeCu30 laser

[8] U.S. Patent No. 6,287,869, Issued Sept. 11, 2001; U.S. Patent No. 6,693,944, Issued Feb. 17, 2004; U.S. Patent No. 7,800,753, Issued Sept. 21, 2010; and U.S. Patent No. 8,395,770, Issued Mar. 12, 2013.

The S11155 CCD array detector, developed, and assumed to be patented, by Hamamatsu Corp., is a back thinned, back illumined, room-temperature linear resistive gate CCD array detector with very high quantum efficiency, near 50%, in the deep to near UV spectral range of interest for the BRANE sensor application. The high resolution fluorescence spectra shown for microbes in Fig. 9 were taken with this new technology detector. This new technology enables the detector array to be read out rapidly, less than about 300 µs, avoiding the accumulation of dark charge and its associated dark noise. This enables the detector to operate at room temperature, something that traditional CCD arrays cannot do since their read out time is very long, typically several ms, a factor of 10 or more. Traditional CCDs require the use of detector cooling to reduce dark noise, which also dramatically increases the power consumption of a system from a few watts to 50 or more watts with related long warm-up times, making a miniature hand-held instrument much more difficult. A remaining problem with the S11155 detector is high read noise, of the order of 30 electrons. Hamamatsu is working to reduce this noise, but we are presently developing spectral averaging methods to alleviate this read noise issue.

During this Phase I effort, we completed the detailed baseline optomechanical design and began construction of the first generation prototype of an instrument that satisfies the goals of the program:
a low-cost, handheld, Biological Reconnaissance & Analysis using Non-Contact Emission-spectroscopy (BRANE) sensor that enables rapid detection and classification of a broad range of suspicious powders in real-time at the site of a contamination incident:

- without the need for reagents, labels, or other consumables;
- without contact with or disturbing the suspicious powder and the subsequent need for decontamination of the sensor or spreading, growing, or dispersing biological threats in suspicious powders.
- Wwith rapid analysis- for each 50 µs laser pulse a full spectrum analysis is possible.
- in a package size about 4" wide by 9" high by 16" deep, weighting less than about 7 lbs.

The layout of the first generation BRANE sensor is shown below in Fig. 11, along with identification of the basic elements.

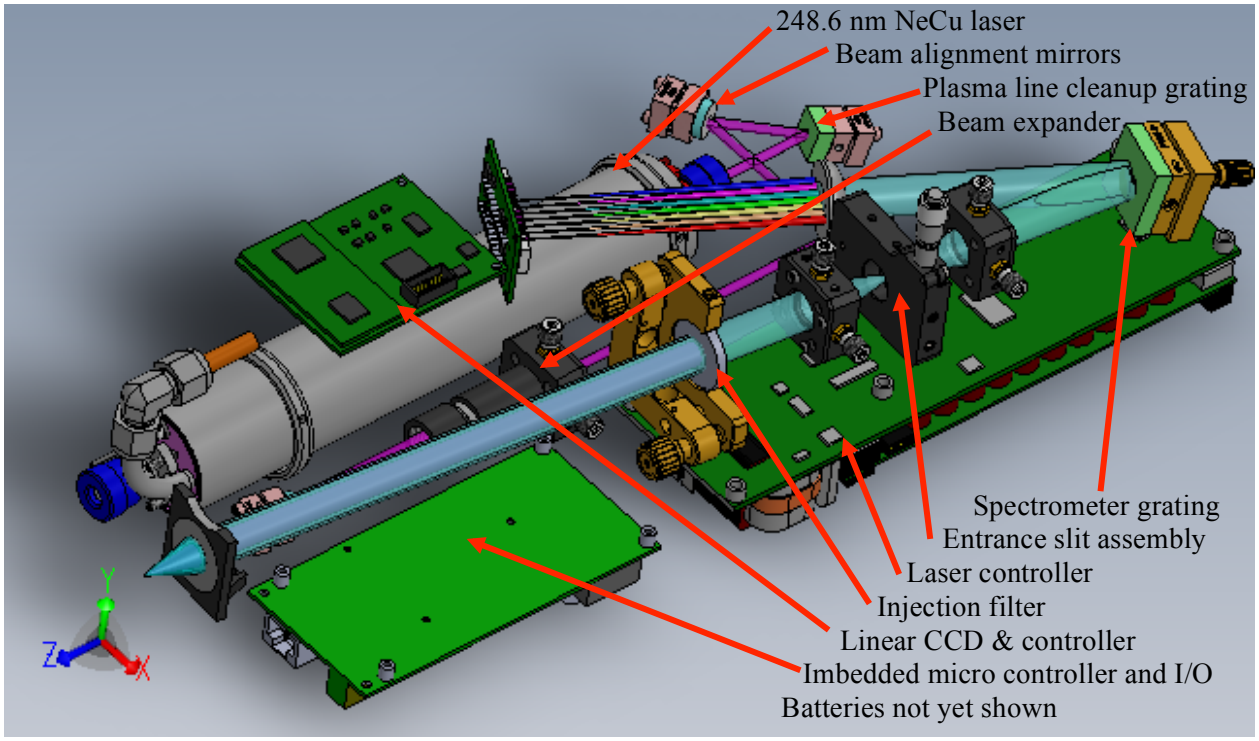

Figure 11. Isometric Solid Works drawing of latest iteration of BRANE sensor design:

This baseline design will likely be modified to reduce the spectra range of detection at the upper end from 430 nm to about 350 nm, both to reduce the effects of ambient lighting as well as to improve the Raman spectral resolution. But, below is the baseline optical and resolution calculations.

- Objective Lens: f/2, 20 mm fl, 10mm aperture. Chromatic design TBD.
- Laser spot size at sample: 4*L*M2*f/Pi*D. L= 0.2486 um, M2=30, f=20 mm, D=8mm (i.e. 3X beam expander). Spot diameter at target, df=23.7 um diameter
- Spot size at spectrometer entrance slit. f/4, 40 mm focal length lens, i.e. 2X spot size or 47.4 um, i.e. **50 um slit**
- CCD Array = Hamamatsu S11155. 2048x1 pixel, 14 um wide by 500 um high pixels. Array size, 28.6 mm wide by 0.5 mm high.
- Spectrometer f/# = 12.5.
- Spectrometer Focal length = 125 mm
- Spot size on CCD array = 125/20 *23.7 um = 148 um
- Number of pixels illuminated = 10.5 pixels
- Dispersion = (430 nm – 248 nm)/2048 pixels = 0.00889 nm/pixel
- Spectral resolution = dispersion/pixel * # of pixels per spot = 0.933 nm or about 150 cm-1 in Raman range. With restricting the higher end of the spectral range from 430 nm to 350 nm, the Raman resolution should improve to about 75 cm-1, which should be sufficient for the specificity desired.

Grating Equations				Army SBIR Suspicious Powders DUV Raman/fluorescence Sensor-BRANE								
				125mm Focal Length		248-430						
beta=asin(-mL/d - sina)												
dL/dx=dcosb/-mf												
Res=L/mN												
Groves/mm			1200		**F/Number**	9.84						
Total Grating Size,mm			12.7		**Total Grating lines**	15240						
Grove Spacing,micr			0.833									
Incidence angle, deg			-55		**Entrance Slit X, mm**	-102.39						
focal length,f,mm			125					**Pract.Res**	**Pract.Res**			
Spectral Order,m			1		**Exit Slit, X**	**X Position**	**Dispersion**	**w 50u slit**	**w 100u slit**	**w 50u slit**	**disp/pixel**	
Wavelength			**beta**	**beta**	**from Normal**	**Spread**	**nm/mm**	0.05	0.1		**14 um**	
Microns	**cm-1**		**Rad**	**degrees**	**mm**	**mm**		**cm-1**	**cm-1**	**nm**	**nm**	
0.2486	**0**		0.548	31.4	65.1	0.0	-5.69	-46.0	-92.1	-0.28	-0.080	
0.257	**1315**		0.536	30.7	63.8	-1.3	-5.73	-43.4	-86.8	-0.29	-0.080	
0.27	**3188**		0.518	29.7	61.9	-3.2	-5.79	-39.7	-79.5	-0.29	-0.081	
0.28	**4511**		0.504	28.9	60.4	-4.7	-5.84	-37.2	-74.5	-0.29	-0.082	
0.29	**5743**		0.491	28.1	58.9	-6.2	-5.88	-35.0	-69.9	-0.29	-0.082	
0.3	**6892**		0.477	27.3	57.4	-7.7	-5.92	-32.9	-65.8	-0.30	-0.083	
0.35	**11654**		0.411	23.5	49.9	-15.2	-6.11	-24.9	-49.9	-0.31	-0.086	
0.4	**15225**		0.346	19.8	42.4	-22.7	-6.27	-19.6	-39.2	-0.31	-0.088	
0.43	**16969**		0.308	17.6	37.9	-27.2	-6.35	-17.2	-34.4	-0.32	-0.089	
0.45	**18003**		0.283	16.2	34.9	-30.2	-6.40	-15.8	-31.6	-0.32	-0.090	
0.5	**20225**		0.221	12.7	27.4	-37.7	-6.50	-13.0	-26.0	-0.33	-0.091	

SolidWorks drawings of the first generation BRANE 1.0 sensor are shown in two views below in Fig. 11. Photos of the first generation BRANE sensor are shown later under Task 4 on p. 26. Figure 11 shows all of the essential elements of the hand held sensor except for the battery and outer housing with handle and display.

At the time of writing of this final report, all of the elements of the baseline first generation BRANE sensor are coming together with final assembly and testing expected to occur during the Phase I Option and Phase II efforts. This is described in more detail under Task 4 below. The basic configuration uses a low thermal expansion, light weight, carbon composite vertical strength member on a horizontal base to maintain all of the optical components in alignment, to provide the platform for mounting all electronics, computers, and battery, and to provide a convenient stand to support all optical, mechanical, and electronics elements and allow easy access for testing and alignment of both sections of the instrument.

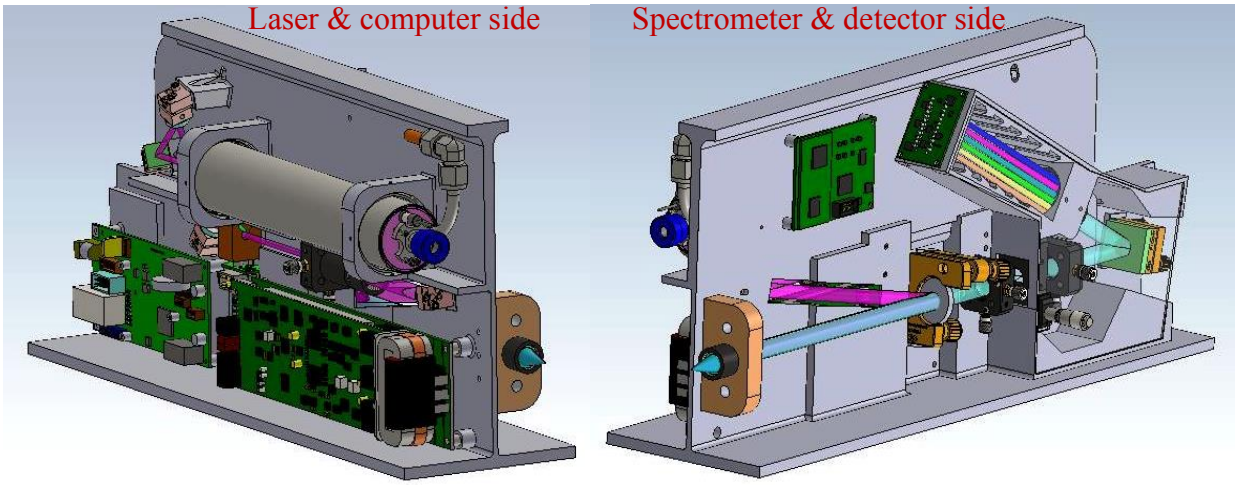

Figure 11. Illustrations of BRANE 1.0 sensor: laser/computer side left, spectrometer/detector side right

The right side isometric view in Figs. 11(left image) above has the laser, laser drive and control electronics, input/output control board with on-board battery charging electronics and imbedded microprocessor and memory for storing all suspicious powder library data and processing all spectroscopic data to compare with library data to determine identity of a suspicious powder, and optical element for processing the laser output. The I/O board will eventually also include an on-board GPS to enable logging of position along with date and time for each data set collected by the BRANE sensor.

The left side isometric view on the right hand side of Figs. 11 has the objective lens, contextual imaging camera (not yet shown), laser injection optics, spectrometer input optics and entrance slit with recollimation optics, grating, spectrometer imaging lens, linear CCD array detector, and detector control and processing electronics.

The laser source illustrated below in Fig. 12 produces about 250 mW at 248.6 nm during a long pulse duration about 50 µs. The laser line is extremely stable with a linewidth less than 2 GHz, corresponding to less than 0.1 cm-1. The laser emission wavelength is insensitive to ambient temperature, shock or vibration, or other external conditions. This eliminates the need for temperature regulation of the laser and related elements and dramatically reduces the need for constant instrument calibration for Raman shift determinations from suspicious powders. These 1 lb lasers are currently at a Technical Readiness Level between 6 and 7, having been tested over a wide range of shock and vibration and ambient temperature and have been deployed on many missions to very harsh environments such as Antarctica, the Artic, and the deep Ocean. We have other programs that will enhance the TRL level of these lasers to TRL 9.

The laser beam exits the laser with a diameter about 2.5 mm. The first optic encountered after output is a grating, G1, above. This 4200 g/mm holographic grating, blazed at 250 nm and with grooves parallel to the mounting plate (plane of page), disperse the output of the laser vertically (out of the page). This grating is in a conical mount with the grating in Littrow configuration in the spectral direction and rotated off axis in the spatial direction to direct the 248.6 nm laser beam to the first turning mirror of the "figure 4" alignment mirrors. This geometry offers nearly 60% throughput of the 248.6 nm laser line. The purpose of G1 is to spectrally separate and eliminate plasma lines and a spurious laser line from the primary laser line at 248.6 nm. The spurious laser line is at 252.9 nm, corresponding to a Raman shift of 683 nm. The primary laser beam is directed to the first and second turning mirrors, which are high efficiency KrF dichroic mirrors with over 99% reflectivity. These KrF mirrors provide the ability to align

the laser beam axis down the center of a 3x beam expanding telescope an on to a third KrF mirror that then sends the laser beam to the left hand, spectrometer side, of the instrument. Also on the right hand side of the instrument is the laser drive and control electronics which incorporate all of the overall instrument control and timing and synchronize the laser pulse with detection electronics and readout of the detector array. This readout is sent to the input/output and Computer board which contains the power conversion for charging and use from on-board battery or external DC power (from the USB port from an external computer), an imbedded microprocessor for data acquisition, processing, data storage, and chemometric algorithms for conversion of spectroscopic information into chemical identification of suspicious powders. In addition, this I/O board contains an on-board GPS sensor which logs the physical position for all spectroscopic and chemical identification information data sets along with a time stamp to form a complete record of all instrument measurements.

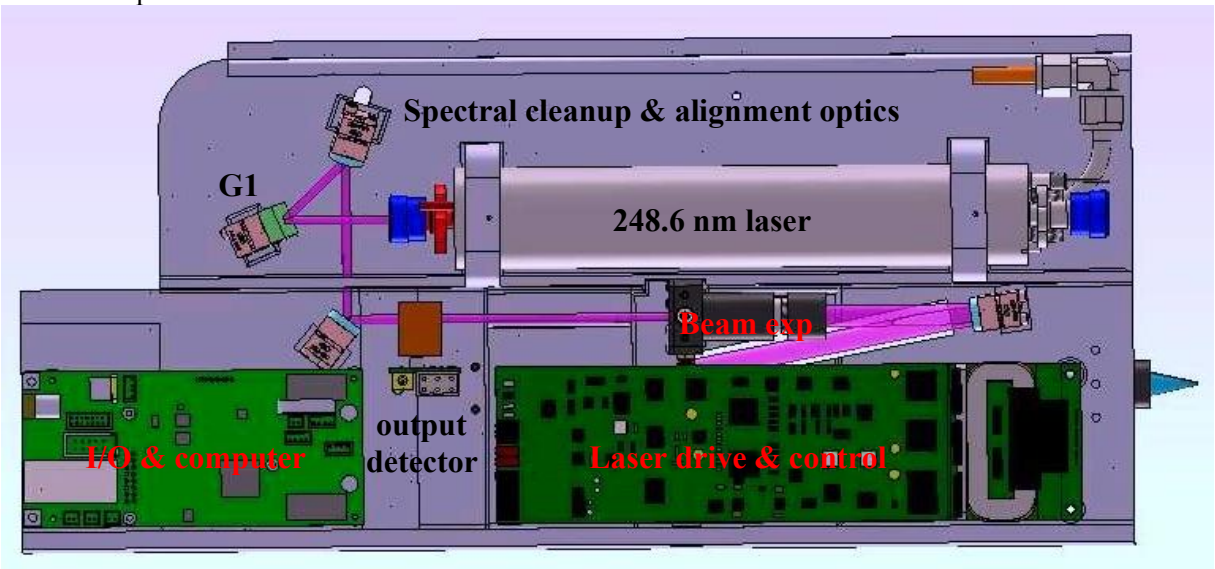

Figure 12. Right side plan view of laser & computer side of BRANE sensor

The fused Raman and fluorescence spectrometer and linear CCD array detector side of the BRANE sensor is shown in plan view in Fig. 13 below.

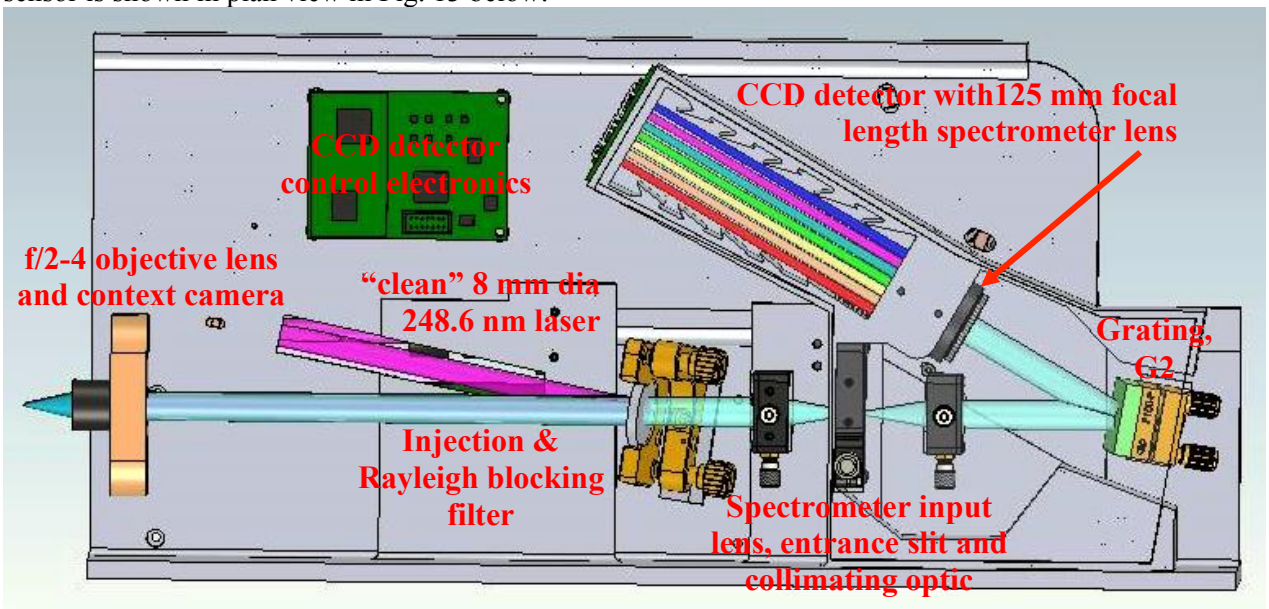

Figure 13. Left side plan view of spectrometer & linear CCD array detector side of BRANE sensor

The "clean" laser beam from the right side of the instrument enters the left side of the BRANE instrument in Fig. 13. The clean laser beam has nearly all interfering emission spectra other than the 248.6 nm laser line. This "clean" laser beam in injected into the optical path from the objective lens to the spectrometer using a customer dichroic filter which reflects the laser wavelength with high efficiency, greater than about 95%, and directs the laser down the axis of the objective lens, which is interchangeable from f/2 to over f/4. With an f/2 objective lens with a working distance about 1.5 cm, the laser excites a spot size about 25 um diameter on the unknown suspicious powder.

The Raman and fluorescence scattered light from the target is then collected by the objective lens and collimated back through the injection filter, which also acts as a Rayleigh blocking filter, reducing or eliminating any transmission of the laser beam toward the spectrometer. The laser beam is then focused using a 40 mm focal length lens into the entrance slit of the spectrograph. We chose this configuration rather than a more efficient slitless spectrometer configuration to provide the greatest level of ambient rejection to enable the BRANE sensor to operate in normal daylight or artificial lighting situations. After the entrance slit, the laser beam is recollimated onto a 1200 g/mm holographic grating blazed at 300 nm, which disperses the light horizontally (in the plane of the page) through a 25 mm diameter spectrograph objective lens which focuses the Raman and fluorescence emissions onto the resistive gate linear CCD array detector. This detector is controlled by customer electronics developed by Photon Systems specifically for this program due to the newness of this detector and lack of availability of alternative detector control electronics which synchronize with the other elements of our BRANE instrument. Next to the objective lens is a contextual imaging camera (not shown) which will provide for focusing of the laser beam on a target as well as providing a visual record of the object that spectral data are being accumulated from. This completes the data base that includes not only the spectroscopic and chemical information about a target, but also its GPS location, time stamp, laser output energy, and other contextual information about the target. This side of the instrument has ample space for a battery to operate the sensor for many hours of field operation.

An illustration of the approximate configuration of the finished BRANE sensor is shown below in Fig. 14. Not shown is the display and controls. Controls would include a simple mechanical on/off button or which, which would power up the basic system, energy the display and preparing the sensor for data taking. Under this standby condition, BRANE will draw battery power about 5W. A trigger in the handle would active the laser and detection electronics and begin taking data on suspicious powders at a rate about 40 combined Raman and fluorescence spectra per second, proving real-time display of the results. For some weak materials it may be necessary to dwell on a sample for up to about 10 seconds although most data are expected to be achieved in less than 1 second.

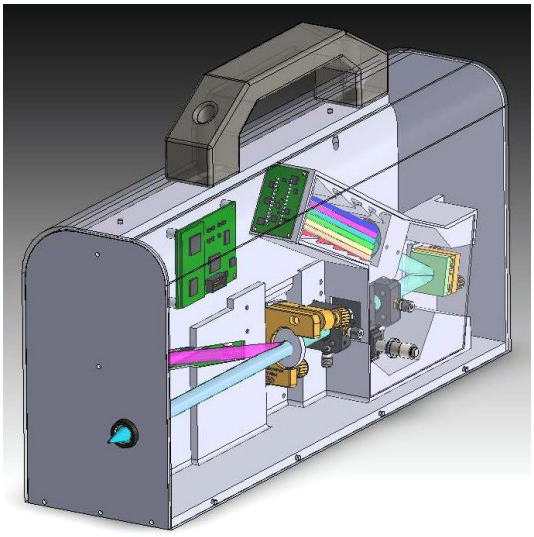

The overall weight is expected to be about 7 lbs and overall size, without handle, about 4" wide by 9" high by 16" deep. The on-board battery is presently planned to be a LIPO with 40 Watt Hours of energy storage, capable of running the sensor continuously, without breaks between samples, for about 2 hours. Since the warm-up time from a completely "off" condition to standby or full power operation is less than 10 s, the expected battery lifetime under normally expected operation would be over 10 to 20 hours, or more. This battery has dimensions of 6" by 2" by ¼", and will fit in any of several locations within the BRANE sensor.

Figure 14. Illustration of packaged BRANE sensor:
7 lbs, 4" wide x 9" tall x 16" deep

Task 3: Control & Analysis Software design of BRANE sensor

The BRANE sensor is a fully independent sensor with all functions on-board for operating the sensor to detect and classify unknown suspicious powders. The basic elements of the sensor are the laser, sample interface and other optics and spectrometer, detector, display, controls, and on-board battery. To control and synchronize these elements there are currently three printed wiring board sets, as illustrated in block diagram, Fig.15, below.

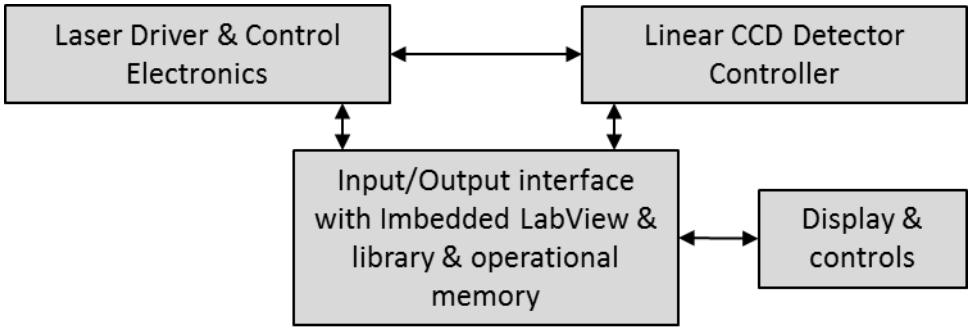

Figure 15. Block diagram of BRANE sensor electronics

Laser Drive & Control Electronics

The laser driver and control electronics (LD) is a COTS board from Photon Systems, used in its commercial laser products. The LD board converts on-board battery voltages to the drive conditions required for the laser, which include an 800 V, 1 μs, ignition pulse followed by a 220 V, 25A drive pulse, which produces about 250 mW of laser output at 248.6 nm during a 50 μs pulse. Pulse repetition rate is typically about 40 Hz during accumulation of a single Raman and fluorescence spectra, which lasts typically less than 1 sec. The average power consumption during spectral accumulation is about 15 W. Power consumption while on standby is about 5 W. At the initiation of each laser pulse, a trigger pulse is sent to the Linear CCD Detector Controller (CD) to enable collection of detected Raman and fluorescence photons to be accumulated in the detector elements, after which the CCD array is read-out in about 200 μs, digitized, and sent to the Imbedded Microprocessor circuit board. The process is traditionally called a gated boxcar integrator, and enables the signal to noise of the detector to be improved by typically over 1000X compared to performing long term integration. A photo of the deep UV laser drive and control electronics are shown below in Fig. 16. This board set currently weights about 1.2 lbs, but a new design with about 1/2 the weight and 1/3 the size is in progress under internal funding.

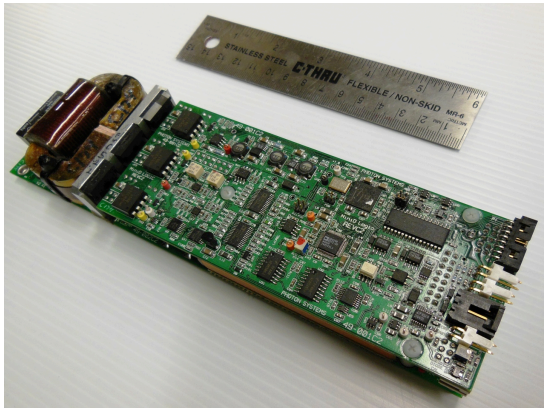

Figure 16. Photo of Photon Systems' deep UV laser drive and control electronics board set.

Linear CCD Array Detector Control Electronics

The linear CCD array detector controller (DC) is a custom set of electronic circuit boards developed on this Phase I contract specifically to control the new technology Model S11155 resistive gate linear CCD array from Hamamatsu. The reason a custom circuit board was needed rather than utilizing a COTS control board from Hamamatsu or elsewhere is that the detector needs to communicate directly with the laser driver & control board and I/O board with imbedded LabView software and real-time memory storage for synchronism of the laser with the detector and with the imbedded microprocessor to enable a smooth flow in data for processing and chemometric identification.

The detector controller is made up of 5 circuit boards: The CCD array detector interface board shown in the upper left corner of Fig. 17 where the Hamamatsu S111555 detector in mounted. The main board shown to the right of the detector interface board contains the timing electronics for the CCD and the interface to the laser drive and control circuit board. And a daughter board mounted on the main board, which contains another microprocessor to synchronize communications with the other boards.

One aspect of the Hamamatsu S11155 detector that is still being improved is the read-out noise, which is currently about 30 electrons and will be reduced over a few years of development to enable even finer spectroscopic features. As a result, we expect the performance of the sensor to continue to improve with time.

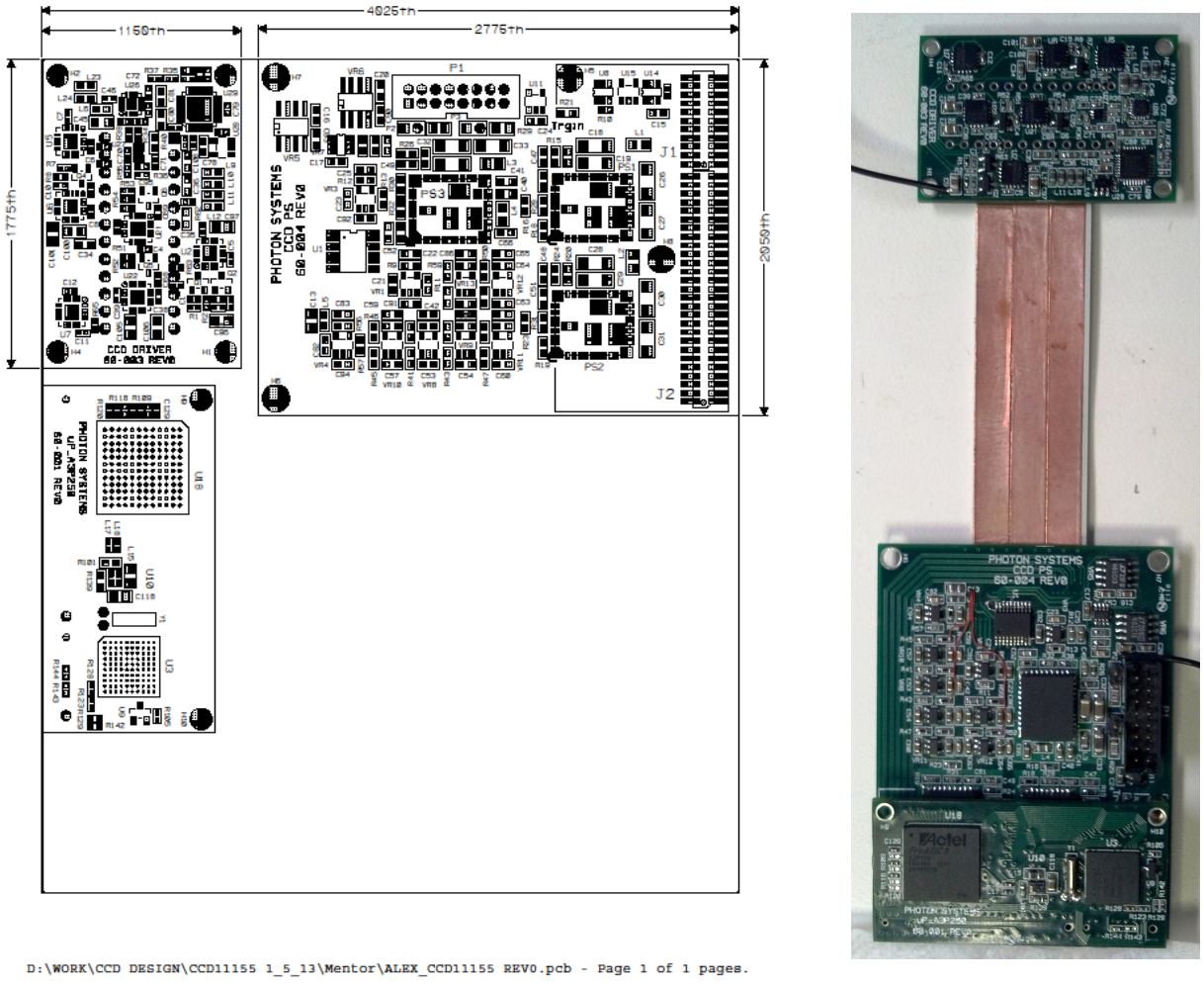

Figure 17. Circuit boards layout and photo of CCD Detector Controller board with laser synchronization

Input/Output interface & imbedded microprocessor electronics

The input/output interface and imbedded microprocessor board is still in evolution. We are presently using a circuit board developed separately which has LabView operating software on an imbedded microprocessor as well as real-time clock and memory for both library chemometric data and chronological data and records during sensor operation and use. What are currently not on board this present I/O interface board is a GPS position indicator, sensor manual control and display interface, and on-board battery charger and controller. We have developed these elements on other programs and will eventually, under a Phase II effort, integrate these elements onto a single circuit board.

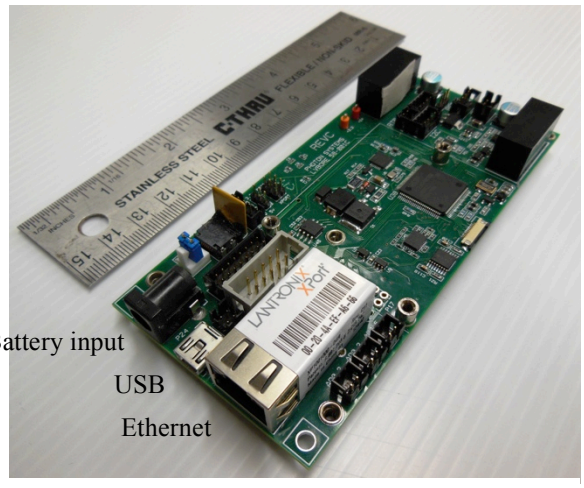

Figure 18. Photo of Photon System' I/O & imbedded LabView board

The on-board LabView software is the heart of the BRANE sensor, providing all of the communication between three different microprocessors which operate the laser, detector, and display. The on-board memory has library Raman and fluorescence spectra of a wide range of suspicious powders. This list of library chemicals was presented in earlier reports.

An example of the graphical user interface (GUI) when using the BRANE instrument with an external computer is shown below in Fig. 19. This GUI shows the output energy of the laser in upper left, a time running indication of the data for any of several Raman and/or fluorescence spectral bands, individual and averaged Raman spectra, and, on the right hand side, a match between data being accumulated and chemical/spectral data in an on-board library for fluorescence, Raman, and combined data sets.

The imbedded board has a LPC2387 ARM7TDMI-S microcontroller running at 12 MHz as the central processing unit. The microcontroller will control and coordinate operation of the LASER and the S11155 Linear Detector. The imbedded board enables the instrument to be run in an autonomous mode without the requirement of an external computer. The LPC2387 microcontroller has the capability to perform real time analysis on the collected data. The data collected will be stored to an on-board micro SD card and can be transferred out using a USB or Ethernet connector. A display connected to the iembedded board will be used to provide feedback on the collected data. The imbedded board can also be controlled using an external computer via RS232 Serial (USB connector) communication or TCP/IP (Ethernet connector) communication.

Primary hardware and preliminary chemometric software issues have been addressed and resolved during the Phase I effort. However, many detailed optical design issues to resolve optical aberration issues, electronic hardware, firmware, and software aspects of the BRANE sensor have not been addressed in Phase I. Many of the hardware aspects of the sensor have been addressed in Phase I. Missing are the battery interface with charger control as well as the GPS. Very little has yet been done regarding a user interface. The basic method of incorporating the suspicious powder data into an analysis as described in Task 1 has not yet begun. This is a very large endeavor. Included in this endeavor is the calibration of the instrument so that an imbedded library is transportable from one sensor to another, to enable a single library to be used on many sensors. Also undone is development of graphical user interface (GUI) is a way that is meaningful to an operator, or a tiered systems for operators at various levels of skill. This is a very large and complicated task.

The format of the present GUI will not be compatible with an on-board display and will need to be simplified. The display can be provided in any of several user defined formats. The basic format will likely only provide information as to the on/off status, data taking, and perhaps a limited list of "names" of the identified suspicious powder. A higher level of display may include the three levels of match with fluorescence, Raman, and combination. Another level or screen may provide more specific information for operators with higher levels of knowledge of chemistry and/or instrument operation.

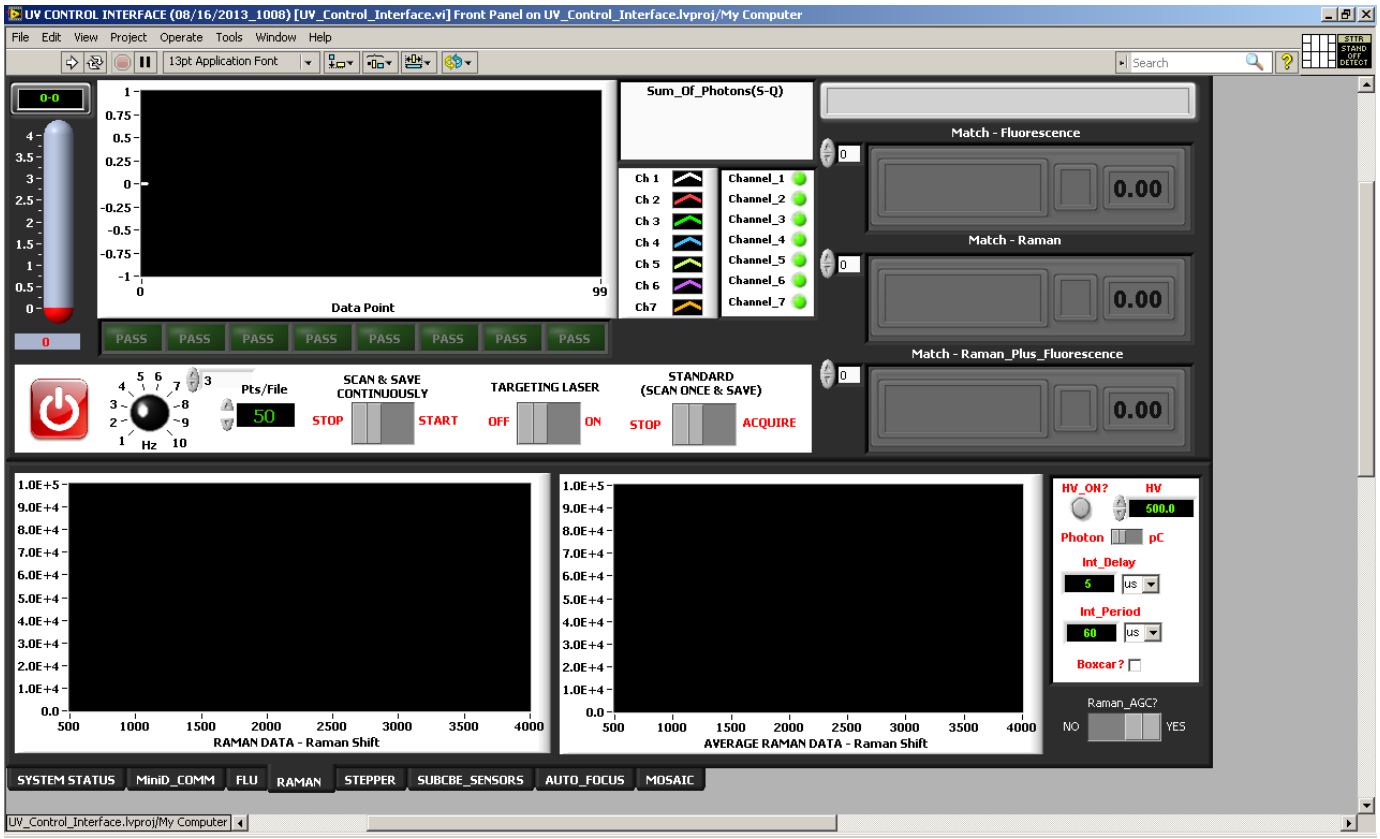

Figure 19. Grapical User Interface for BRANE sensor operating on external computer

Task 4: Fabricate a first generation BRANE sensor

Under this task we will develop a breadboard version of the BRANE sensor. This task will incorporate the output of Task 2 to provide a design that is optimal for bacterial detection and classification.

The BRANE 1.0 sensor design has been sent to a rapid prototyping supplier on Sept. 30, 2013 for generation into hardware as illustrated in Fig. 11. This hardware was being populated with a laser, laser drive electronics and all other optical and mechanical components during October 2013 before this final report in early November 2013. This design and subsequent testing will form the basis for our Phase I Option and Phase II efforts, which will be to test this design and begin the process to refine the design of optical element to maximize spectral resolution and instrument sensitivity as well as to refine the firmware and software to incorporate an on-board library of known suspicious powders and improve algorithms for matching unknown Raman and fluorescence spectra with library data to optimize and provide a robust method of identifying targets. In addition, the BRANE 1.0 sensor will for form the baseline for testing the sensor for shock, vibration, and thermal ruggedness. It is expected that one or more iterations of the design will be needed to develop and demonstrate a working, fieldable, prototype by the end of the Phase II contract.

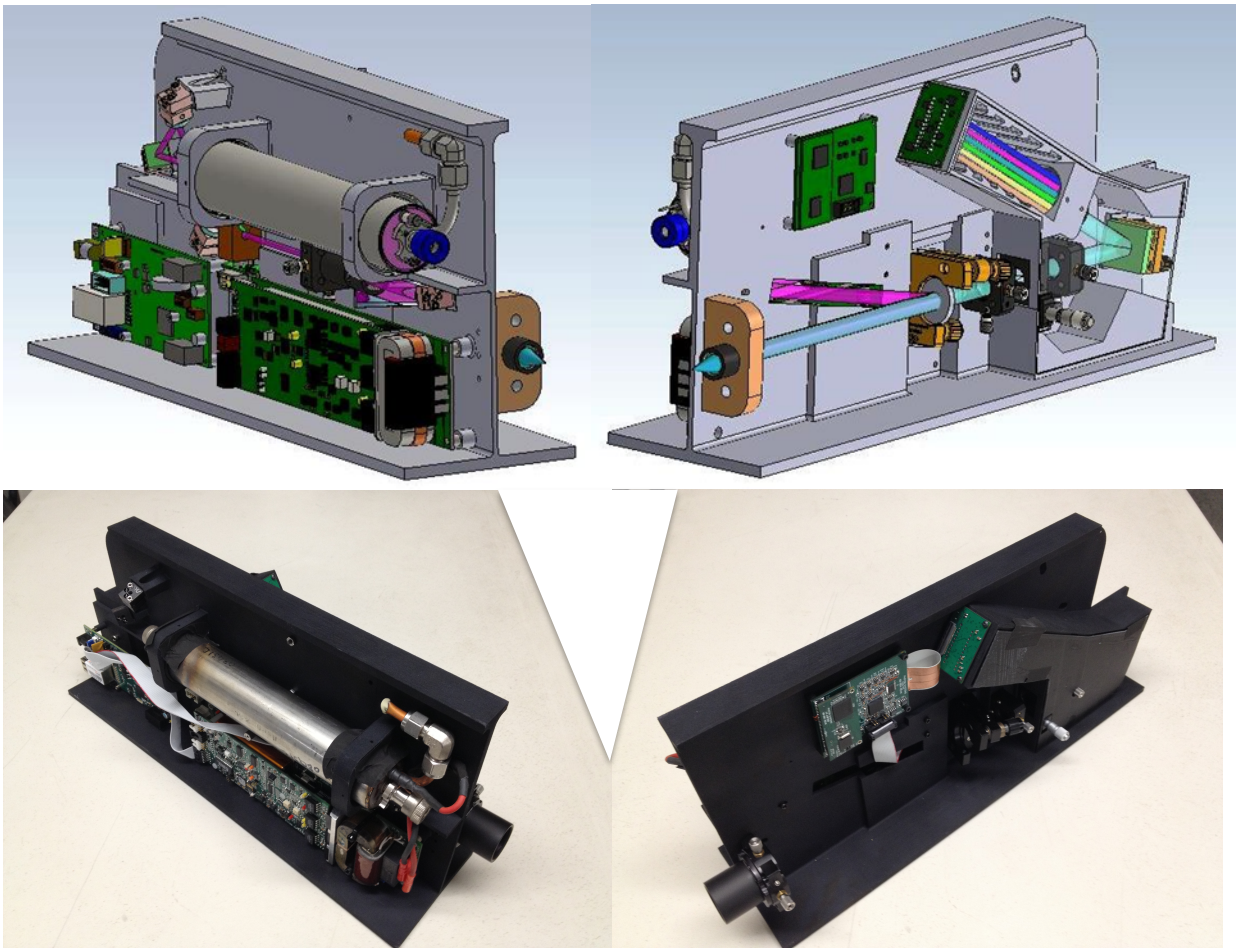

Figure 20. Comparison SolidWorks illustrations and photos of first generation BRANE sensor: laser/computer side left, spectrometer/detector side right with most key elements physically in place.

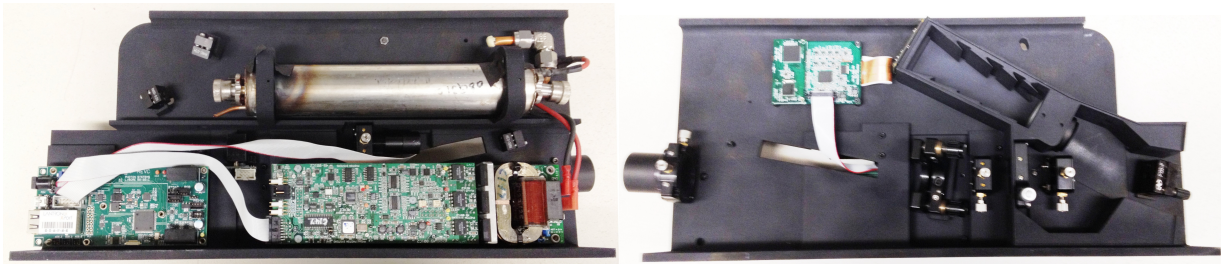

Figure 21. Plan view of both sizes of first generation BRANE sensor

Appendix A: Preparation of microbial samples

A.1 General Issues of Sample Preparation

Preparation of sample is critical to these experiments. Although in real-world environments microbes will be mixed with a variety of interferents, when testing to demonstrate the ability to differentiate microbes it is important to ensure that the samples are what we think they are and they are "pure" or "clean" and do not contain interferents. This is also true for all chemical samples tested during this Phase I effort. Chemical can be purchased with high levels of "purity". Microbes, on the other hand, cannot. We have purchased specific microbes in the past and found that the samples typically contain a wide range of foreign material other than the microbe. Therefore we followed the procedure below for preparation of these microbial samples.

A.2 Protocol for microbial washing

1mL of bacterial cells were grown up in LB media and put into micro-centrifuge tubes. The tubes were centrifuged at 14000 RPM for 5 min and the supernatant was discarded. The cells were re-suspended in in 1 mL of M9 media, vortexed, and centrifuged again at 14000 RPM after which the supernatant was discarded. This was done 3 times to remove traces of LB. The cells were then re-suspended in 10μL of M9 media to provide a small droplet size needed for spectroscopic testing. We have found that the fluorescence of M9 media is much lower than the typical 1% NaCl media for washing.

A.3 Protocol for microbial solid/solid dilutions in talc

This describes the preparation methodology for microbial samples diluted in a solid-solid matrix of dispersant, such as talc. The goal is to determine feasibility to distinguish bacteria from a background powder. Four different bacteria were used to run this test: Bacillus atrophaeus, Bacillus subtilus, Escherichia coli, and Pseudomonas aruginosa. Each microbe was mixed with talc to yield a 1:1000 microbial to inorganic ratio, based on weight. The average weight of a single bacterial cell is $1x10^{-12}$ g or $1x10^{-9}$ mg. Therefore the desired mixture ratio would be 1 mg of cells per 1000 mg of talc, or 0.01 mg of cells per 10 mg of talc. The number of bacteria to be mixed in talc to achieve the 1:1000 ratio is shown below in Table A1 for different masses of talc.

Table A1. Cells required for 1:1000 cells to talc mass ratio

Mass talc (g)	Mass talc (mg)	Required # of cells
1000	1000000	$1.0x10^{12}$
10	10000	$1.0x10^{10}$
0.1	100	$1.0x10^{8}$
0.01	10	$1.0x10^{7}$

Each microbial sample was counted using a haemocytometer under an Olympus BX51 microscope with 40x objective lens in bright field, and the concentrations of stock solutions are shown in Table A2.

Table A2. Microbial concentrations

Sample	Microscope count (unwashed)	Unwashed (cell counts/mL)	Microscope count (washed)	Washed (cell counts/mL)
E. coli	127	6.40E+09	30	1.50E+09
P. aruginosa	42	2.10E+09	19	9.50E+08
B. subtilus	27	1.30E+08	22	1.10E+08

To provide a 1:1000 solid/solid dilution of microbes in talc, E.coli and P. aruginosa required 100 μL of suspended microbes in 100 mg of talc. B. subtilis required 100 μL of suspended microbes in 10 mg of talc.

To provide a 1:100 solid/solid dilution of microbes in talc, E.coli and P. aruginosa required 1 mL of suspended microbes in 100 mg of talc. B. subtilis required 1 mL of suspended microbes in 10 mg of talc.

Each of these solid/solid dilutions were formed on 500C baked stainless steel plates, as shown in Fig. A1 below.

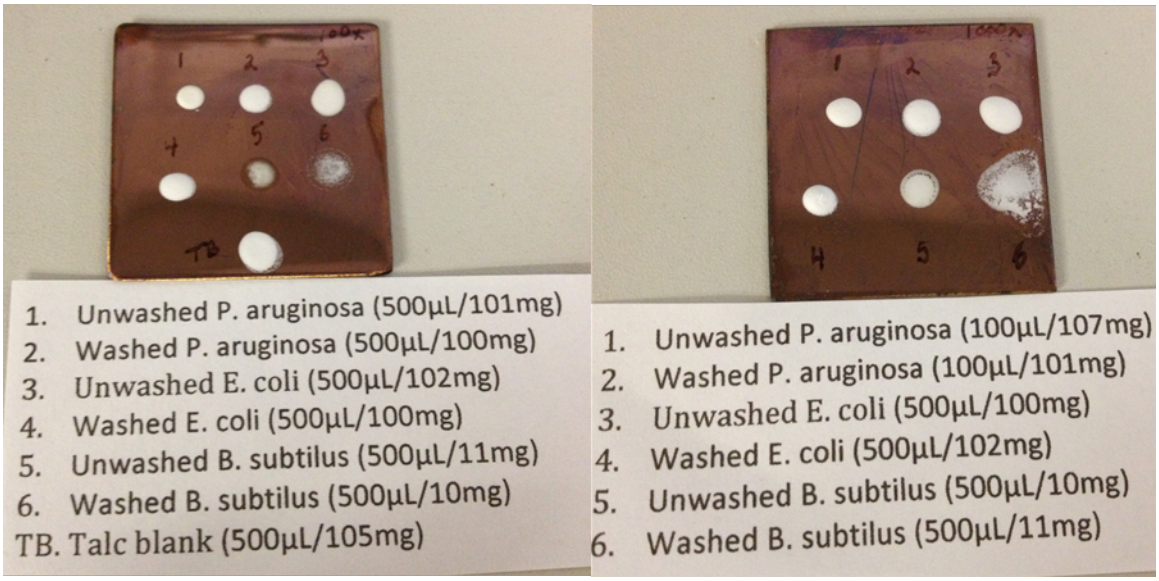

Figure A1. Photo of baked stainless steel plates with solid/solid mixtures of microbes in talc dried down onto plates. Left: 100x, Right: 1000x. Numbers denote volume (μL) cell suspension dropped per weight talc (mg)

Appendix B: Deep UV Raman & Fluorescence Spectral Data

In an effort to better understand which spectroscopic mode or modes are needed, bacteria, proteins and will be analyzed and compared using a custom laboratory high spectral resolution fused deep UV Raman and native fluorescence instrument that resides in the labs of Photon System. We used this instrument to determine the effect on bacterial specificity of Raman and fluorescence spectral resolution, laser spot size, objective f/number, and working distance. These parameters have a direct impact on the size, weight, ruggedness, and cost of the sensor. Initially we will be testing only benign microbes. But we also have access to BSL 2 laboratories in which to test hazardous bacteria and biotoxins at some future date.

Below, in Fig. B1, is a photo of the custom deep UV Raman and fluorescence spectroscopic instrument at Photon Systems. This instrument was developed separately but is being used here to provide preliminary data with which to optimize the design of the BRANE instrument proposed for this contract.

This custom instrument shown below employs a 248.6 nm NeCu laser manufactured by Photon Systems as well as custom filters and optics needed for use in the deep UV. This laser is the primary enabling components of the eventual hand-held instrument being developed here. The enabling feature of the laser is not only that it emits at an important wavelength below 250 nm, but also that the laser linewidth is narrow enough to enable simultaneous Raman and fluorescence measurements on unknown suspicious powders. In addition, the laser weighs less than about 1 pound and consumes less than about 5 W of electrical power. In addition, laser cost is nearly 100 times less than other lasers operating below 250 nm.

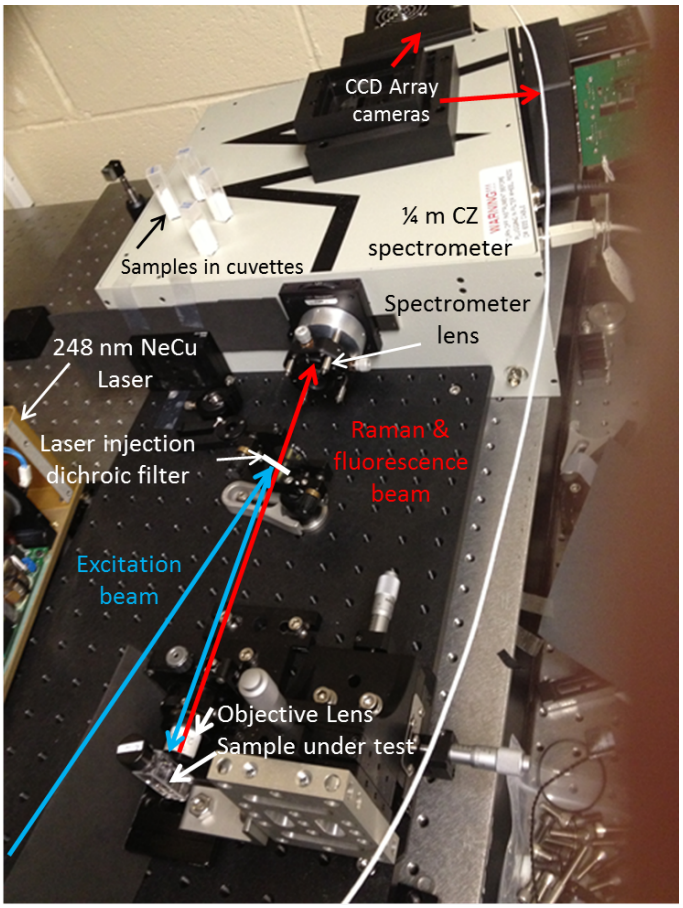

Figure B1. Illustrated photograph of custom deep UV Raman and fluorescence spectrometer

Only the edge of the laser is shown in Fig. B1. The laser beam has clean-up optics (not shown) to eliminate unwanted plasma lines and a spurious laser line at 252.9 nm, corresponding to 683 cm-1 in Raman spectral terms. This then provides a clean single wavelength for excitation of the sample. The laser is then injected into the spectrometer path by the "laser injection dichroic filter" which reflects the laser energy into the optical path between the sample and the spectrometer. This filter reflects the laser wavelength with high efficiency (reflectivity) but efficiency transmits wavelengths above the laser wavelength.

The laser energy is then focused onto a sample by the objective lens shown at the bottom of Fig. B1. This objective lens has a visible focal length of 20 mm and a deep UV focal length about 18 mm. This produces a laser excitation spot size on the sample about 50 μm diameter, producing Rayleigh scattering (at the laser wavelength), Raman scattering (associated with chemical bonds of compounds within the laser spot, and fluorescence emissions from the sample excited within the laser spot diameter and related volume within the sample. The Raman and fluorescence emissions from the target are collected from the sample at f/1.8 and collimated through the dichroic injection filter to a spectrometer focusing lens that images the laser spot on the sample onto the entrance slit of the spectrometer. The visible focal length of this lens is 50 mm. In the deep UV, the focal length is about 45 mm. The laser spot on the sample is magnified 2.5X so the image spot on the entrance slit is about 125 μm diameter. The entrance slit used for the following data was 120 μm wide, allowing nearly all of the light from the excited sample into the spectrometer. These spot diameters assume the use of diffraction limited optics for both the objective lens and the spectrometer focusing lens. Presently these lenses are simple fused silica singlets and are not diffraction limited. We are purchasing better lenses and will integrate them into a upgrade of this instrument along with a microscope imaging camera.

Two different spectrometer focal plane array detectors are mounted on this spectrometer: a Hamamatsu C7042, 2-stage thermo-electrically (TE) cooled 1024x64 element CCD array detector, operating at -20C; and a Fingerlakes Inc. Camera with 3-stage TE cooled 2048x122 element CCD array detector operating at -40C. This camera was recently mounted so the data shown below are entirely from the C7042 Hamamatsu camera.

A combined spectra of powdered sugar, granulate sugar, fruit pectin, flower, corn starch, baking powder, baking soda, aspirin, Aleve, and acetaminophen are shown in Fig. B2 below. The spurious laser line at 683 cm-1, corresponding to a wavelength of 252.9 nm is shown. The remaining lines are due to the list of powders listed above. Most of the spectral information occur in the region from about 750 cm-1 to 2000 cm-1

Along with the Raman data, fluorescence emissions from each target material were taken. This is shown below in Fig. 3 for the same set of materials as in Fig. 2. The Raman data provides information regarding the existence of specific chemical bonds within the sample. Fluorescence data provide information about the overall molecular structure of the sample. As discussed in the proposal, fluorescence is typically many thousands of time more efficient than Raman and thereby can provide information about the chemical nature of a sample at much lower concentrations and in much shorter periods of data collection time than Raman. The combined method, which has been patented by Photon Systems, provides a much probability of false alarm than either method alone.

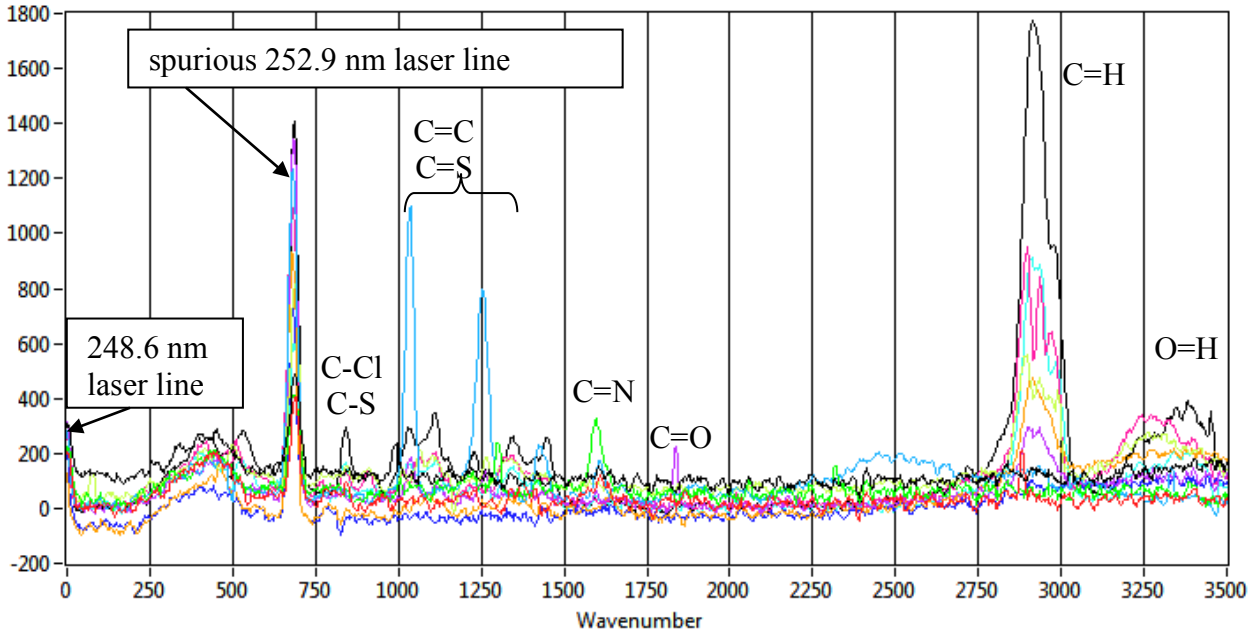

Figure B2. Combined Raman spectra of interfering white powders: powdered sugar, granulate sugar, fruit pectin, flower, corn starch, baking powder, baking soda, aspirin, Aleve, and acetaminophen

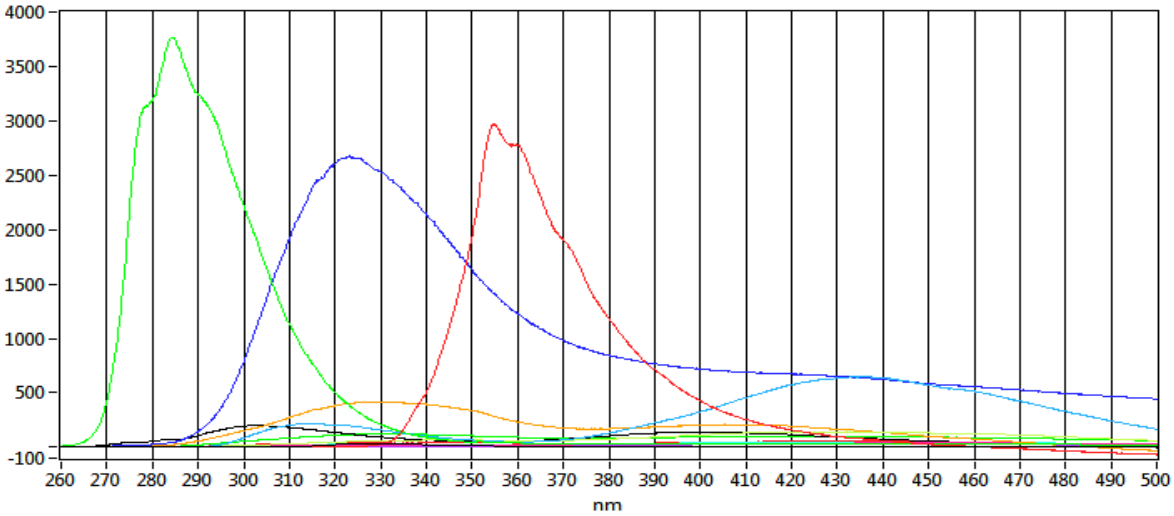

Figure B3. Combined fluorescence spectra of interfering white powders: powdered sugar, granulate sugar, fruit pectin, flower, corn starch, baking powder, baking soda, aspirin, Aleve, and acetaminophen

Figure B4 below shows the same data as in Fig. B3, but with an expanded vertical scale to demonstrate the variety in the fluorescence spectral distribution of the various interfering powders.

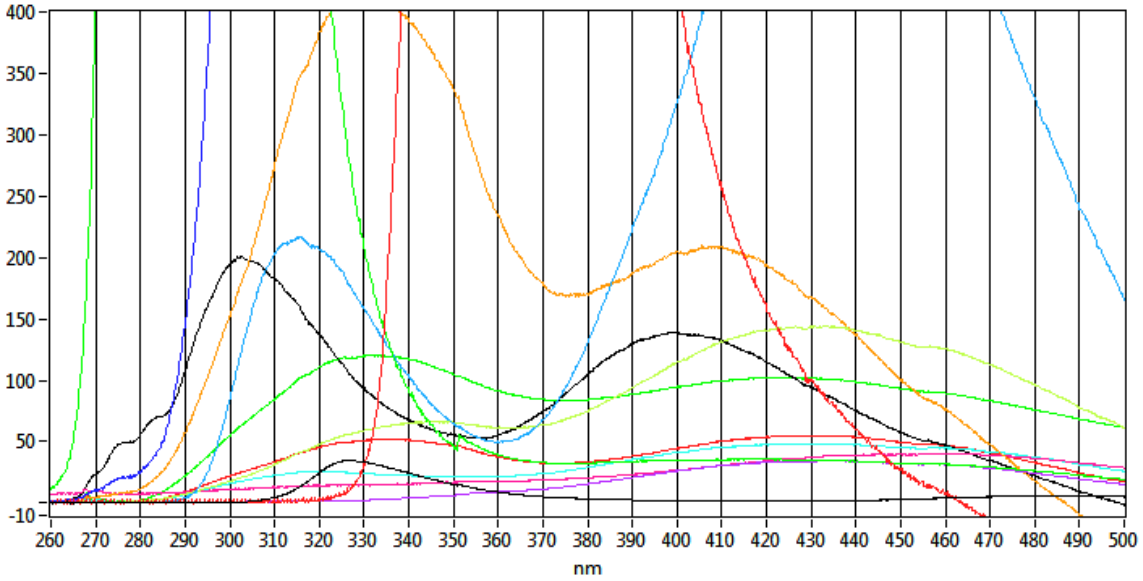

Figure B4. Combined fluorescence spectra as in Fig. 3 but with expanded vertical scale.

75 mm focal length spectrometer data: room temp S11155 detector

As will become clearer using better detectors below, the Hamamatsu S11155, although inexpensive, low power consumption, and low weight, is not a good detector for measuring Raman spectra on microbes. This is illustrated in Fig. B5 below, where the data are normalized to 1 at the band or peak at 2250 cm-1. This is traditionally the N2 line in air and not associated with microbes. However, there appears to be a doublet band near 1600 to 1700 cm-1, which is a strong Raman region for microbes, indicating these spectra may not be just noise.

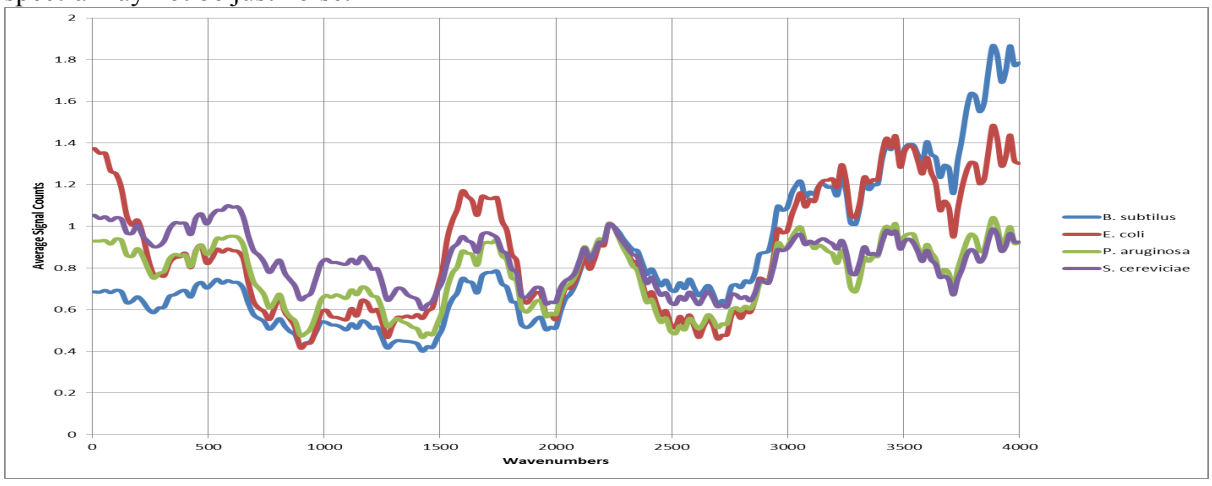

Figure B5. Raman spectra of microbes using room temperature S11155 detector

The spectral resolution of the above Raman spectra is poor because this spectra was taken on the same S11155 CCD array detector as the fluorescence spectra, and at the same time. The spectral resolution for the fluorescence is excellent and for the Raman poor since at the Raman wavelengths the relationship between cm-1 and nm is about 160 cm-1/nm. Thus, an excellent 1 nm fluorescence resolution is only a poor 160 cm-1 Raman resolution.

We can improve this situation in the final BRANE design by limiting the spectral range of the spectrometer to 250 nm to 350 nm (a delta of 100 nm) instead of the present 240 nm to 510 nm, a delta of 270 nm, improving both the Raman and fluorescence spectral resolution by nearly 3x to a resolution in the range of 60 cm-1. The major problem with using this detector for Raman will remain dark and read noise for the weak Raman signals.

260 mm focal length spectrometer data: 3-stage TE cooled detector

Our 260 nm Oriel spectrometer system also employs a Photon Systems' 248 nm NeCu laser and a 3-stage thermoelectrically cooled 2048x122 element E2V CCD array detector operating at about -35C. Raman spectra, shown below in Fig. B6, were taken of the same microbes as for the 75 mm focal length spectrometer shown in Fig. B5 above. Note the dramatic difference in SNR and clarity of the spectra. The Raman bands near 1600 cm-1 and 1700 cm-1 appear to be merged together in the Raman spectra of Fig. B5 because of the lower resolution of the 75 mm instrument, although the fact that they seem to be present at all with the S11155 detector is remarkable, and gives hope for its incorporation in the BRANE sensor. The other major Raman peak in Fig. 5 is at 1400 cm-1, which does not show up in Fig. B5. The legend below Fig. B6 indicate which spectra are associated with each microbe.

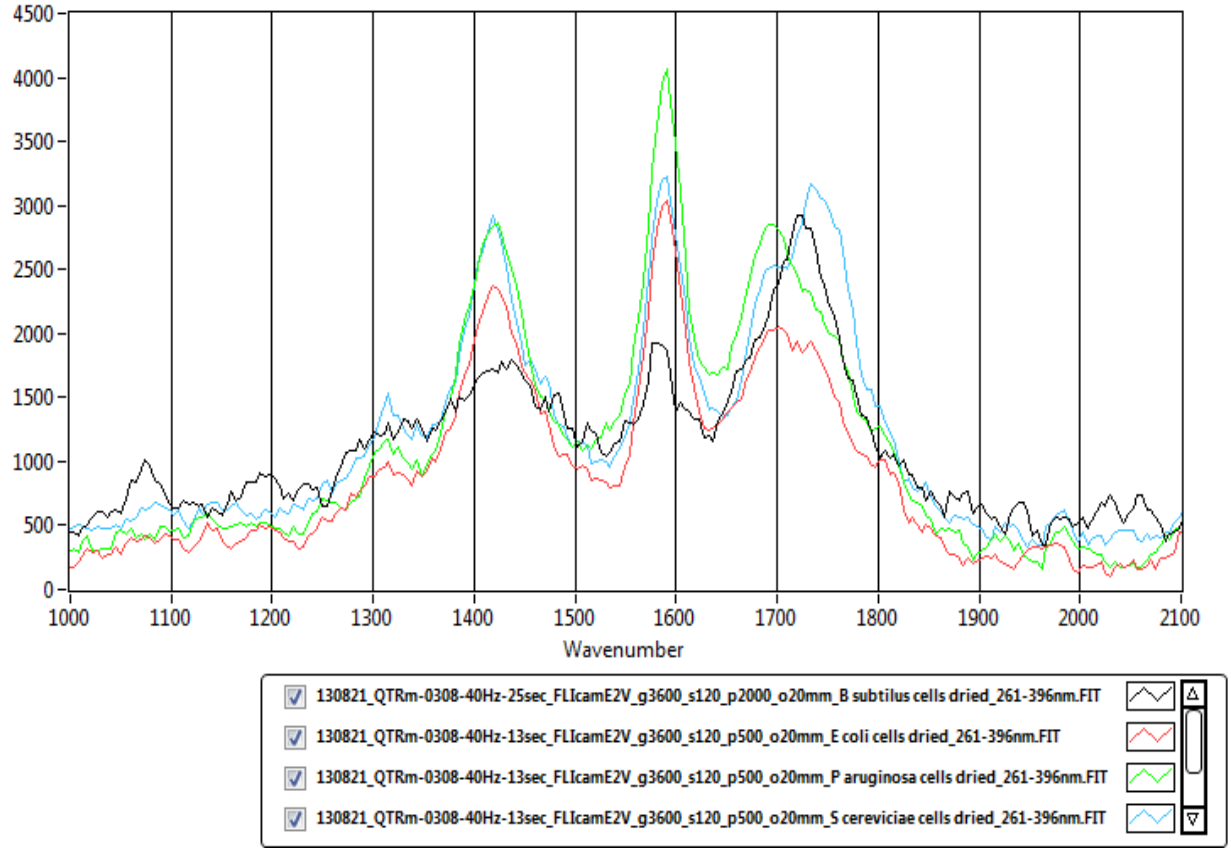

Figure B6. Raman spectra of 4 microbes using a 260 mm focal length spectrometer with 3-stage cooled CCD array camera with detector operating at -35C

550 mm focal length spectrometer data: LN2 cooled detector

Below, in Fig. B7, are the Raman spectra of four bacteria using the 550 mm focal length spectrometer fitted with a liquid nitrogen cooled CCD array camera. These spectra are considerably different from the spectra with the 260 mm spectrometer shown in Fig. B6 above. Although the nitrogen line in Fig. B7 below shows up where expected at 2250 cm-1, the bacterial Raman bands are considerably different from those in Fig. B6 We are looking further into this. We do not believe it is related to a spectral calibration

since all spectra on the 260 mm instrument are spectrally calibrated against an acetonitrile spectrum with each data set.

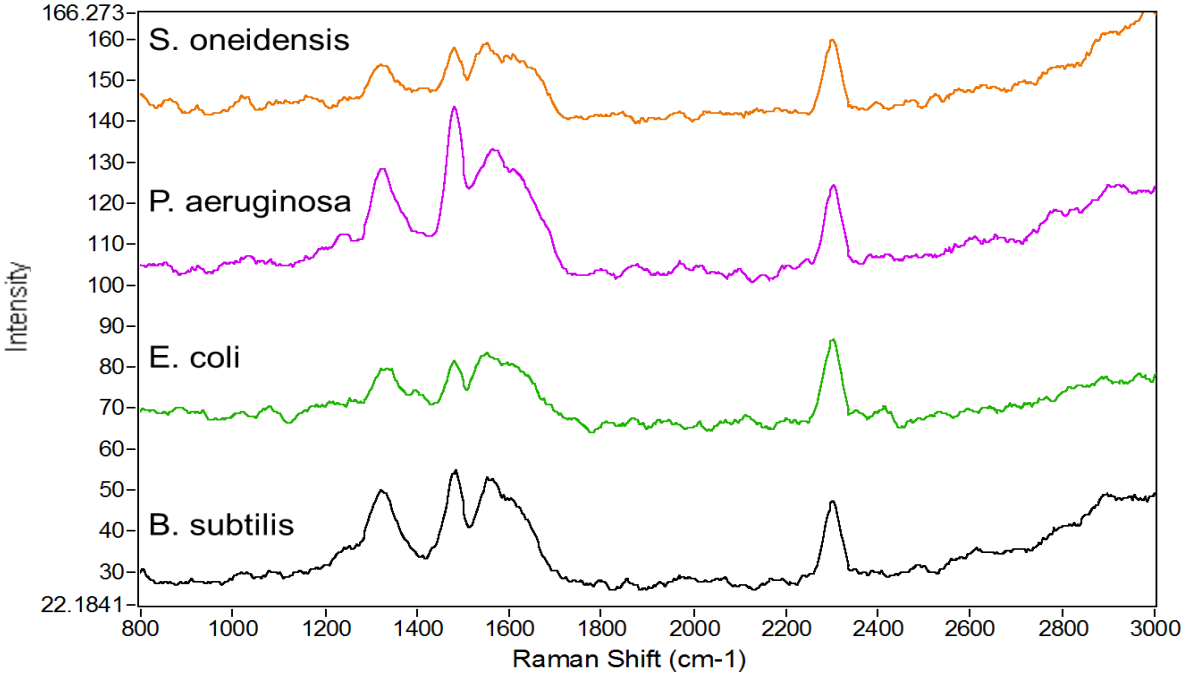

Figure B7. Raman spectra of bacteria taken on the 550 mm spectrometer with LN2 cooled CCD

We are looking into difference in the preparation of the samples as well as inoculation and drying times to understand the effect on the differences in these data sets.

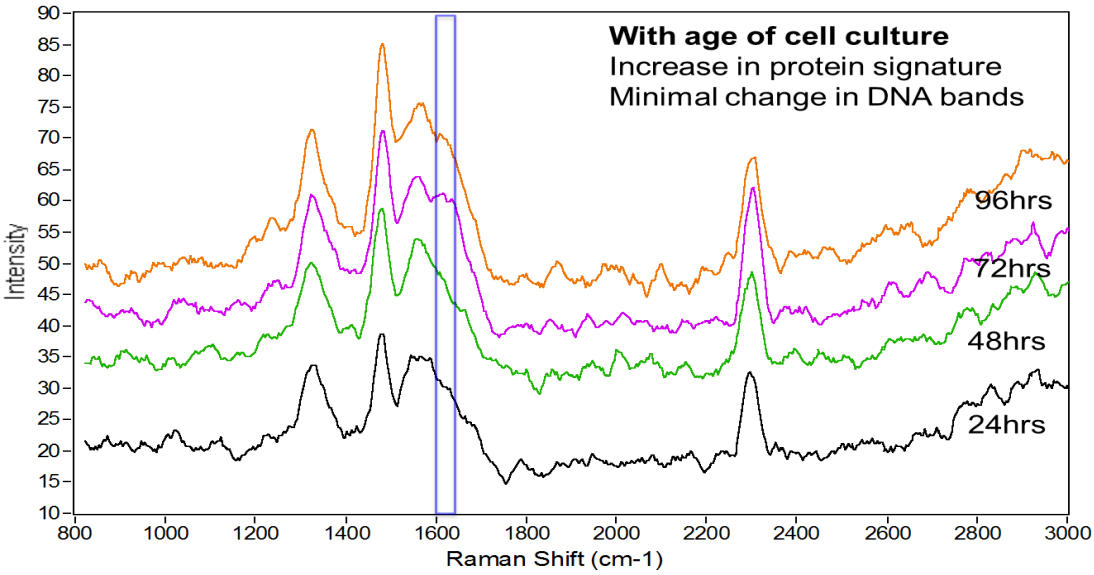

Figure B8. Raman spectra of single bacterial culture as a function of innoculation time

Samples prepared for testing on the 550 mm instrument were primarily grown in M9 media, which alters the chemistry of bacteria by limiting their growth. Most of the data taken on the 260 mm instrument used samples grown in LB media, a much more nutritious diet, leading the larger and healthier bacteria. The table below shows the variations in the different bacteria for which Raman and fluorescence spectra were taken.

Fluorescence data taken on the 550 mm instrument, shown last month, also showed some differences with the present data shown in Fig. B3 and B4 above. We are also looking to understand what difference growth media, inoculation time, and drying time may have played in these differences.

Table BI. Bacterial sample preparation parameters for Raman and fluorescence data

Cell	Media Type	Innoculation Time (Hrs)	Dry Time (Hrs)	Plate Number	RAMAN Data Taken	Fluor Data Taken
Bacillus subtilis	LB	24	24	1		
Bacillus subtilis	M9	24	24	3		
Bacillus subtilis	M9	48	48	4		
Bacillus subtilis	M9	96	4	6		
Bacillus subtilis	M9	72	2	8		
Bacillus subtilis	M9	96	2	10		
E. Coli	LB	24	24	1		
E. Coli	M9	96	6.5	5		
E. Coli	M9	72	2	9		
E. Coli	M9	96	2	11		
Psedomonas aeruginosa	LB	24	24	2		
Psedomonas aeruginosa	M9	24	24	3		
Psedomonas aeruginosa	M9	48	1.5	4		
Psedomonas aeruginosa	M9	48	48	4		
Psedomonas aeruginosa	M9	96	4	6		
Psedomonas aeruginosa	M9	24	4	7		
Psedomonas aeruginosa	M9	72	2	8		
Psedomonas aeruginosa	M9	96	2	10		
Shewanella oneidensis	LB	24	24	2		
Shewanella oneidensis	M9	96	6.5	5		
Shewanella oneidensis	M9	72	2	8		
Shewanella oneidensis	M9	96	2	10		
Control	LB	24	24	1		
Control	M9	48	48	4		
Control	M9	96	6.5	5		
Control	M9	72	2	9		
Control	M9	96	2	11		
Stainless Steel	LB	24	24	1		

Distribution:

- Dr. Stephanie A. McElhinney, Program Manager, Biochemistry, ARO (Stephanie.a.mcelhinny.civ@mail.mil)
- https://extranet.aro.army.mil,
- usarmy.rtp.aro.mbx.reports@mail.mil.